Extension and Subsidence of the Eastern Snake River Plain, Idaho

David W. Rodgers,[1] H. Thomas Ore,[1] Robert T. Bobo,[2]
Nadine McQuarrie,[3] and Nick Zentner[4]

ABSTRACT

The deformational history of the eastern Snake River Plain (SRP) is interpreted from rocks, structures, and landforms within and adjacent to it. Crustal extension is manifested by west-dipping normal faults that define a half-graben fault style along the north and south margins of the plain. Cumulative extension averages 15-20 percent and diminishes only slightly from the south margin to the north, evidence of no lateral shear beneath the plain. Miocene-Quaternary volcanic and sedimentary rocks fill the half grabens and provide evidence of two pulses of extension that migrated northeast through time. One pulse of minor extension began 16-11 Ma and ended 11-9 Ma, and a second pulse of major extension began 11-9 Ma and lasted a few million years in any one location as it migrated eastward to the eastern edge of the Basin and Range, where it continues today. Because many Miocene faults project into the eastern SRP with no evidence of diminishing offset, normal faults are interpreted to have characterized the eastern SRP in middle and late Miocene time. Since then, upper crustal extension has been accommodated primarily by mafic dike injection.

Subsidence of eastern SRP rocks relative to Basin and Range rocks is manifested by the accumulation of a thick volcanic succession, crustal flexure of its margins, and marginal normal faults. Northeast-striking marginal normal faults only accommodated 2-5 percent extension associated with crustal flexure, not downfaulting of eastern SRP crust. Crustal flexure along the northern margin of the eastern SRP is evidenced by Cretaceous fold hinges whose southward plunges increase regularly toward the plain. Isoplunge contours define a zone of flexure about 20 km wide that accommodated 4.5-8.5 km of subsidence of eastern SRP rocks. Age-depth relations of eastern SRP volcanic rocks indicate 1.7 km of rock subsidence since 8.0 Ma, 3.1 km since 8.5 Ma, and the initiation of subsidence before 10 Ma.

Subsidence of the eastern SRP surface relative to the Basin and Range surface is manifested by axial drainage that extends 50 km beyond the SRP margins. Streams that are tributary to the Snake River have deeply incised Basin and Range valleys along the southern margin of the eastern SRP, a process attributed to SRP surface subsidence and consequent base level lowering of the Snake River. The age and amount of surface subsidence are recorded by a strath terrace near Pocatello that cuts across tilted 7.3-Ma basin fill and is perched 900 m above the modern plain. Drainage reversals at tributary stream headwaters provide evidence of ongoing Pleistocene subsidence.

Space-time patterns of extension and subsidence are used to support a three-stage model of deformation. Stage 1 involved minor half-graben normal faulting and possibly regional subsidence of the proto-eastern SRP. Stage 2 involved regional rock subsidence and major extension via normal faulting. Extension was focused slightly east of coeval silicic magmatism, and both migrated northeast after 11 Ma. Deformation and coeval magmatism were widely dispersed across the plain at about 10 Ma. Stage 3 has involved ongoing rock subsidence, surface

Editors' note: The manuscript was submitted in June 1998 and has been revised at the authors' discretion.

[1]Department of Geosciences, Idaho State University, Pocatello, ID 83209-8072
[2]595 Ford Road, McKenzie, TN 38201
[3]Division of Geological and Planetary Sciences, California Institute of Technology, Pasadena, CA 91125
[4]Department of Geology, Central Washington University, Ellensburg, WA, 98926

Rodgers, D.W., H.T. Ore, R.T. Bobo, Nadine McQuarrie, and Nick Zentner, 2002, Extension and subsidence of the eastern Snake River Plain, Idaho, *in* Bill Bonnichsen, C.M. White, and Michael McCurry, eds., Tectonic and Magmatic Evolution of the Snake River Plain Volcanic Province: Idaho Geological Survey Bulletin 30, p. 121-155.

subsidence after about 7 Ma, and extension via dike injection after about 4 Ma. Stage 3 deformation has been located west of coeval silicic magmatism.

Key words: Yellowstone, Snake River Plain, Basin and Range, extensional tectonics, lower crustal flow, crustal subsidence

INTRODUCTION

The eastern Snake River Plain (SRP) is a bimodal magmatic province with little surficial evidence of crustal deformation. A few basaltic rift zones, rare normal faults, and a relatively low regional elevation are the only indication of crustal movement. In contrast, the adjacent Basin and Range Province is characterized by a relatively high regional elevation and widespread normal faults that accommodate both crustal extension and vertical offset. Structural and geomorphic features clearly indicate that different deformational processes are currently operating in the two provinces, but what causes the differences and what defines the transition remain difficult to discern. The two provinces also experienced temporal changes in deformation style and kinematics. The eastern SRP evolved during the past 16 Ma through a complicated process of magmatism and deformation, but little is known about the Neogene deformational history during the eruption of voluminous rhyolites and the early stages of basaltic magmatism. Neogene rocks and structures of the eastern SRP that probably record this earlier history are concealed beneath Quaternary basalts.

Fortunately, footwall uplifts of the adjacent Basin and Range contain rocks and structures that record several pulses of late Cenozoic deformation. Some pulses were restricted to the Basin and Range, whereas others were more extensive and affected what is now the eastern SRP. The late Cenozoic rocks have been studied by some workers, notably Kirkham (1927, 1931), Trimble (1980), Trimble and Carr (1976), Allmendinger (1982), Kellogg (1992), Pierce and Morgan (1992), and especially Anders and his coworkers (Anders and others, 1989; Rodgers and Anders, 1990; Anders and others, 1993; Anders, 1994) who used the tectonic tilts of Neogene rocks to interpret that the locus of Basin and Range faulting migrated eastward and away from the eastern SRP through time.

Similarly, we have worked in late Cenozoic rocks of the Basin and Range, but we have focused along the eastern SRP margins where structures, basin fill, and geomorphology record deformation that may have affected the eastern SRP. Results indicate that crustal extension and subsidence occurred in the eastern SRP throughout the Neogene and that deformation was intricately tied to the rise of magma, its accumulation within the crust, and the space-time pattern of eruptions. Our objective in this paper is to document the Neogene and Quaternary deformational history, the space-time pattern of deformation and magmatism, and the landscape evolution to develop an evolutionary model of eastern SRP deformation. Most of the data and interpretations in this paper were first presented in Master's theses by Zentner (1989), Bobo (1991), and McQuarrie (1997) who worked under the supervision of D.W. Rodgers and H.T. Ore. Except for some abstracts and one paper (McQuarrie and Rodgers, 1998), the information was not widely disseminated or integrated, a situation this paper attempts to rectify.

STRUCTURAL SETTING

A complicated pattern of crustal extension has affected the eastern SRP region (Figure 1). The eastern SRP itself appears relatively unextended with just a few late Quaternary volcanic rift zones presumed to overlie mafic dikes. Neogene to early Quaternary structures are completely obscured by younger basalt flows. Beyond the eastern SRP are normal faults of the Basin and Range Province, some of which are active as indicated by arcuate zones of high topography, high seismicity, and high to moderate Quaternary slip rates that are almost symmetrically distributed about the eastern SRP. Most workers attribute the modern extensional pattern to the Yellowstone magmatic system and its interaction with the southwest-drifting North American plate, though the actual mechanics of this process are unclear. To better understand the interaction between extension and magmatism, a few workers have studied the older Neogene history of normal faults near the eastern SRP. Anders and others (1989, 1993) measured the ages and rates of faulting both north and south of the eastern SRP, and interpreted them in terms of a migrating "seismic parabola" shaped like the modern one. Rodgers and others (1990) compiled the space-time relations of SRP magmatism and faulting south of the SRP and proposed a model of concomitant tectonic activity, wherein the SRP experienced crustal extension (via normal faulting, ductile attenuation, and magma injection) before, during, and after magmatism at any one locality. Recent studies, in particular new dating and correlation techniques, have revised data and interpretations concerning the space-time pattern of extension. One goal of this paper is to present information that will explain the interaction of extension and magmatism on the eastern SRP.

Perhaps as unusual as the pattern of crustal extension is the pattern of subsidence in the eastern SRP. First recognized by King (1878) as "a depressed area which subsided very gently with minimal faulting" (Kirkham,

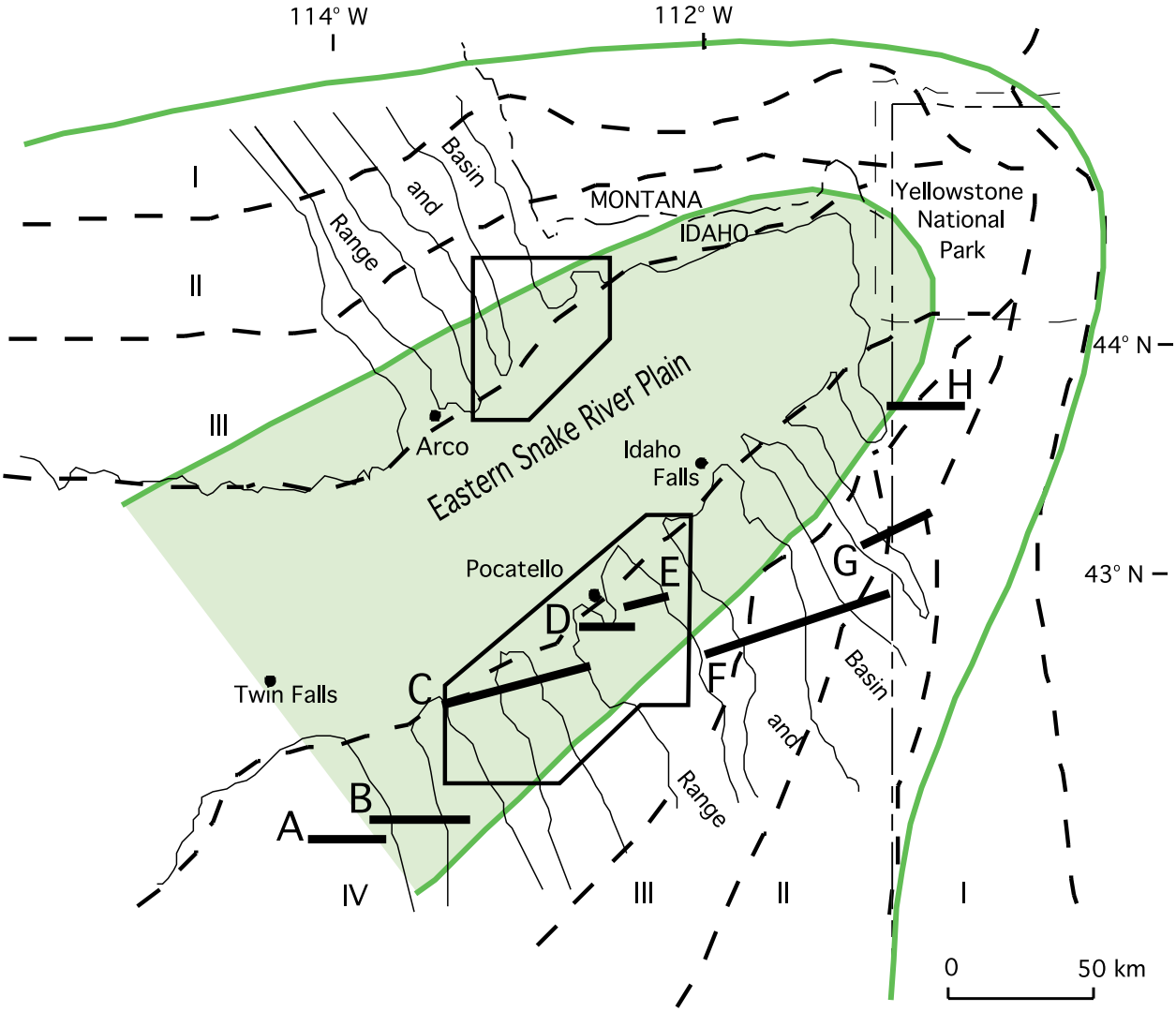

Figure 1. Geography and tectonic domains of eastern SRP and adjacent Basin and Range Province. Dashed lines divide Quaternary fault zones (I, II, III, IV) of Pierce and Morgan (1992). Gray lines define seismic parabola of Anders and others (1989). Polygons indicate locations of study areas shown in Figure 2. Lines labeled A-H indicate locations of composite cross section shown in Figures 3 and 4.

1931), the eastern SRP shows over 2 km of topographic relief and as much as 8 km of structural relief (McQuarrie, 1997) compared to adjacent regions. Surface subsidence is also apparent within the eastern SRP, as manifested by a southwestward decline in elevation along its axis. Brott and others (1981) proposed that thermal contraction in the wake of a hot spot was an important subsidence mechanism, and Leeman (1982) proposed that crustal densification by mafic magma was significant. Quantitative subsidence analyses were performed by a few workers, notably Brott and others (1981) and Anders and Sleep (1992), who studied along-axis subsidence, and McQuarrie and Rodgers (1998) who studied cross-axis subsidence. A useful approach adopted in the latter study was to consider the eastern SRP a basin, similar to sedimentary basins, such that its margins record flexure and faulting associated with basin formation and that its volcanic fill records the subsidence history. Although our basin analysis of the eastern SRP is still underway, initial results (Zentner, 1989; McQuarrie and Rodgers, 1998) suggest a close relation between subsidence and crustal densification by mafic magma. In this paper, we discuss the subsidence record and available age constraints to aid in understanding the space-time pattern of eastern SRP intrusive activity.

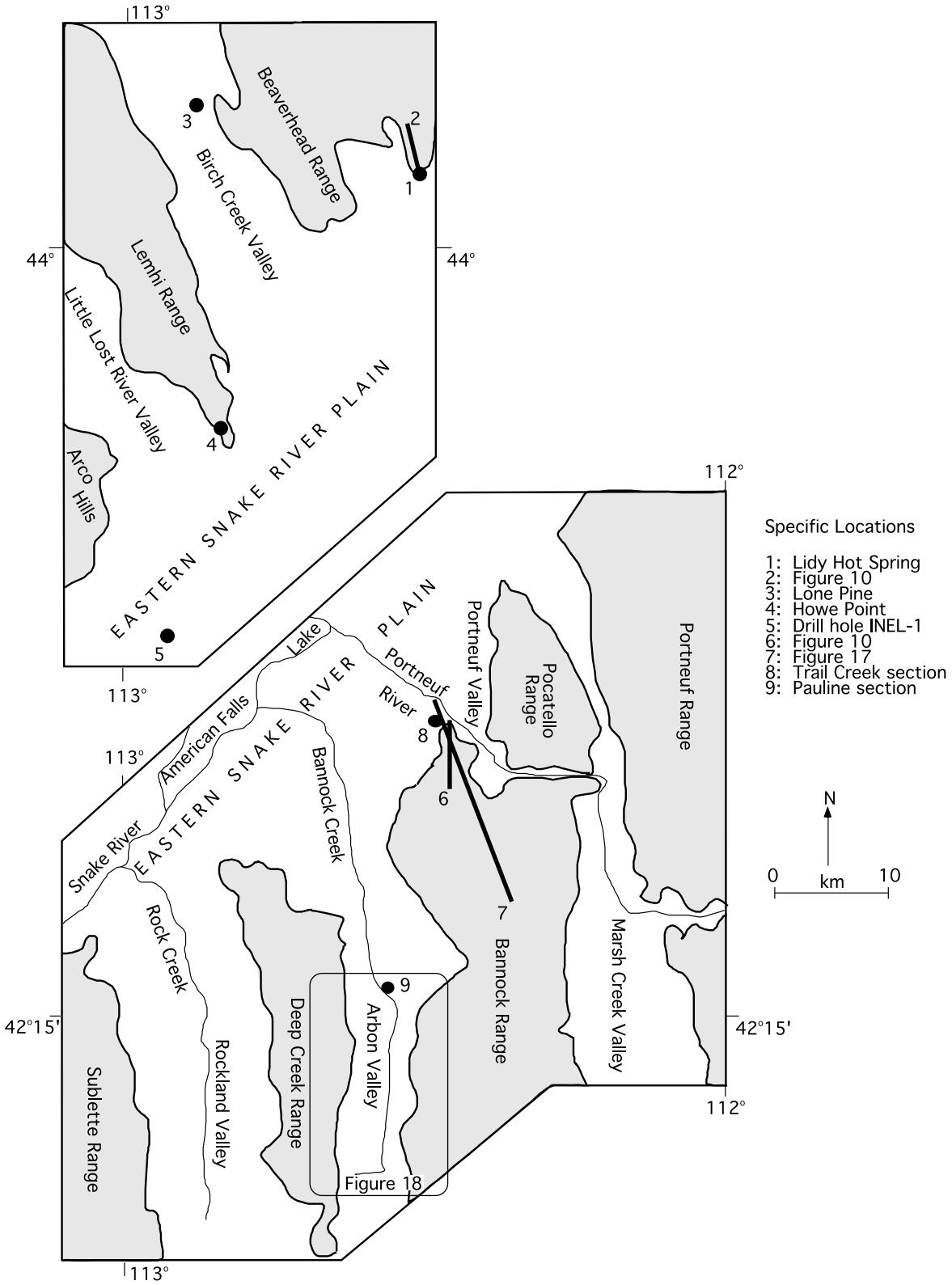

Figure 2. Geographic maps along the north and south margins of the eastern Snake River Plain showing geographic features and specific locations mentioned in text. Location of maps shown in Figure 1.

CRUSTAL EXTENSION

The eastern SRP is surrounded by extended crust of the Basin and Range Province. Nowhere along the plain margins have any workers identified eastern SRP-parallel strike-slip faults, orographic bending, or minor pull-apart basins that would indicate abrupt termination or lateral offset of the Basin and Range faults. Until such structures are found, it must be inferred that the eastern SRP crust experienced a kinematic history similar to that of the adjacent Basin and Range Province.

Normal faulting and dike injection are two processes that accommodated much of the eastern SRP extension. Dikes were the main means by which Pliocene-Quaternary mafic magma rose from mantle through the crust (Kuntz, 1992). Basaltic dikes are not observed in the eastern SRP today but are inferred from Quaternary volcanic rift zones that cut across the eastern SRP (Kuntz and others, 1992). Their absence at the surface today merely reflects ongoing subsidence and accumulation of younger volcanic rocks.

Large normal faults are similarly not observed on the surface of the eastern SRP. We interpret, however, that they exist at depth beneath the plain, because faults in the surrounding Basin and Range project directly into the plain and timing relations (discussed below) suggest many faults were active before basalt magmatism commenced on the plain. To understand this early phase of extension, we have studied the Miocene history of Basin and Range faulting and then projected it into the eastern SRP.

PLIOCENE-QUATERNARY EXTENSION OF THE EASTERN SNAKE RIVER PLAIN

Late Quaternary volcanic rift zones are present on the eastern SRP and are interpreted to overlie basalt dikes that accommodated crustal extension (Kuntz and others, 1992; Kuntz, 1992; Hackett and others, 1996). The rift zones are parallel to the Basin and Range faults and in places are nearly colinear with them. Rodgers and others (1990) first proposed that dike emplacement was the main extensional mechanism in the Pliocene-Quaternary eastern SRP, and Parsons and Thompson (1991) and Parsons and others (1998) provided analytical evidence that dikes could accommodate a similar amount of extension as that along adjacent Basin and Range faults.

Quaternary volcanic rift zones are concentrated in the northern half of the eastern SRP but are uncommon in the southern half (Kuntz and others, 1992). We suggest that this pattern reflects along-strike changes in Quaternary strain magnitude similar to those in the adjacent Basin and Range Province (Anders and others, 1989; Pierce and Morgan, 1992). The actively extending northern half of the eastern SRP is compatible with Pierce and Morgan's (1992) fault zone III along the northern margin of the eastern SRP, and the relatively inactive southern half of the eastern SRP is compatible with fault zone IV along the southern margin of the eastern SRP where normal faults are inactive (Pierce and Morgan, 1992). This view of Quaternary deformation makes the Snake River the axis of the regionally extensive zones of seismicity and Quaternary extensional activity, such that these patterns are symmetrically distributed about the modern Snake River. In this interpretation, the margins of the eastern SRP are thought to mark a fundamental change in extensional style but not a significant change in extensional kinematics.

MIOCENE EXTENSION OF THE EASTERN SNAKE RIVER PLAIN

The eastern SRP extensional history before basaltic magmatism is speculative because the older structures are concealed beneath younger basalt. However, normal faults along the north and south margins of the eastern SRP are exposed. They provide a record of Miocene deformation that can be extrapolated beneath the eastern SRP, a procedure justified by the absence of plain-parallel strike-slip faults and the geometry of crustal flexure (McQuarrie and Rodgers, 1998; and described below).

Basin and Range Faults South of the Eastern Snake River Plain

The style and kinematics of Basin and Range extension south of the eastern SRP were studied by compiling geologic maps and cross sections into one regional cross-section (Rodgers and others, 1994; Figures 3 and 4). Because the goal was to extrapolate extension into the eastern SRP, the section was located close to the eastern SRP wherever extensive, high quality mapping was available. The construction of each cross section is described in Figure 3, and the regional style and kinematics of faulting is summarized below. The age of faulting is addressed in a subseqent section on basin fill.

Extension occurred along normal faults that generally define a half-graben style. Nearly all normal faults dip 25º-60º W. Most faults with small offset dip more steeply, and faults (or fault sets) with more offset dip more gently, evidence of domino-style tilting during fault slip. Some faults, like the Grand Valley fault and Aspen Range fault, are influenced by older west-dipping thrust ramps (Royse and others, 1975). Other west-dipping faults may have been controlled by other west-dipping thrusts (e.g.,

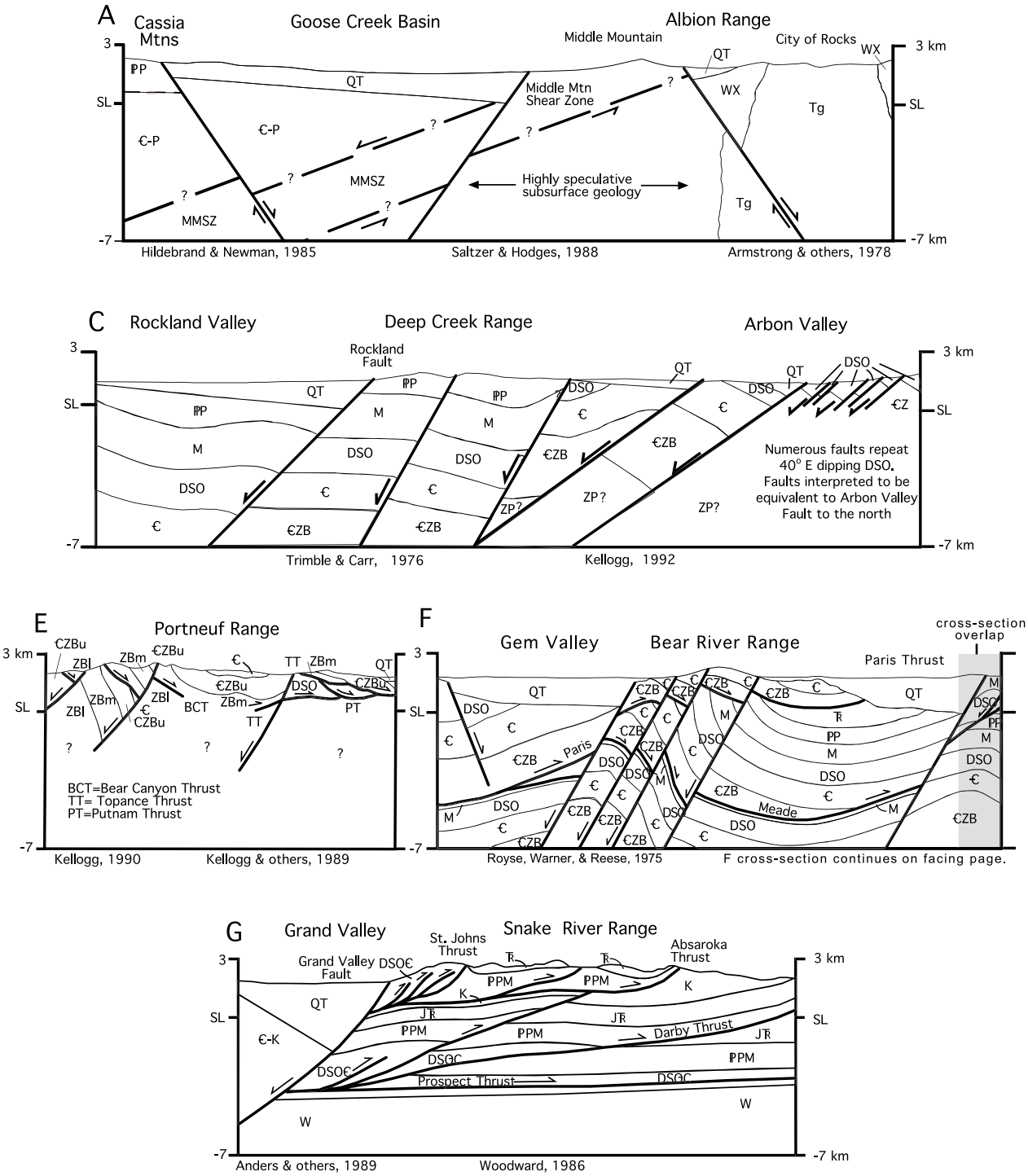

Figure 3. Cross sections of Basin and Range south of the eastern Snake River Plain, showing geometry and style of faulting. Location of cross sections shown in Figure 1. From Rodgers and others (1994) and compiled from sources listed below cross sections.

Figures 3A and 3B. The western end of the cross section is in the Cassia Mountains which bound the Owyhee Plateau, a relatively unextended middle Miocene rhyolite plateau. The Albion Range is a metamorphic core complex flanked by two different detachment faults, the Eocene-Oligocene Middle Mountain shear zone (with rocks metamorphosed at 20+ km; Saltzer and Hodges, 1988) and the early to middle Miocene Raft River fault (with 25 km slip; Covington, 1983). West of the Albion Range is the relatively unextended middle Miocene Goose Creek Basin and to the east is the middle Miocene Raft River Valley. Space problems associated with the contrasting detachments have not been addressed in this cross section.

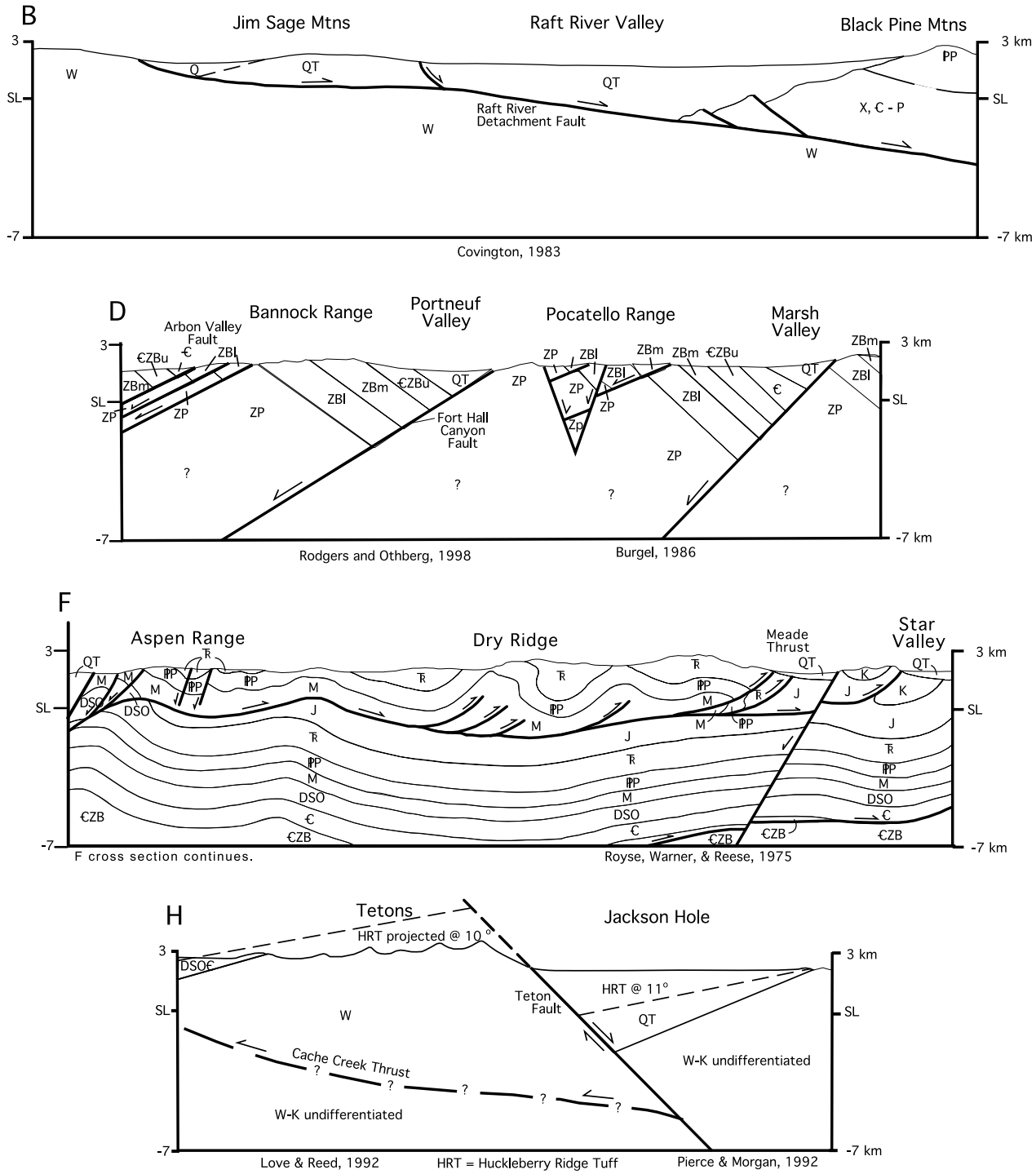

Figure 3C. One major fault lies within the Deep Creek Range, and one borders it on the west. Early(?) to middle Miocene rocks in Rockland Valley dip gently east, whereas bedrock and early(?) to middle Miocene rocks in Arbon Valley dip more steeply east. The fault geometry in Arbon Valley is not well-characterized: Trimble and Carr (1976) show repeated sections of Paleozoic bedrock plus Miocene basin fill that we have reinterpreted to be bounded by several west-dipping normal faults. The overall westward decrease in age of exposed bedrock in Arbon Valley was interpreted by Rodgers and Janecke (1992) to reflect a concealed Mesozoic thrust ramp. Two problems remain in this section: whether the Raft River detachment exists at depth, and whether the geometry of the fault in western Arbon Valley is correct (because the fault shows major slip without forming a deep basin).

(Caption continues on the next page.)

Figures 3D and 3E. Late Proterozoic to Middle Cambrian rocks are exposed in the Bannock Range and Pocatello Range. These once deep-seated rocks were probably uplifted twice, first along a ramp of the Mesozoic Putnam thrust (whose deep structure is unknown and not shown) and later along Miocene normal faults (Rodgers and Janecke, 1992). The normal faults are more gently dipping (25-45 degrees) than faults elsewhere in the regional cross section. The comparatively shallow basins may reflect prolonged uplift above regional base level or the close spacing of normal faults. The Portneuf Range is cut by normal faults, but the dominant structure is a duplex system associated with the Putnam thrust (Kellogg and others, 1989; Kellogg, 1990).

Figure 3F. This cross section is only slightly modified from Royse and others (1975), who recognized a few normal faults superimposed on Mesozoic thrust faults. Normal faults in the Bear River Range are shown as uniformly west-dipping, though Royse and others (1975) show a few east-dipping faults. The location of the normal fault that bounds the Aspen Range may have been determined by a footwall ramp in the Meade thrust.

Figures 3G and 3H. Anders and others (1989) proposed 4 km of middle to late Miocene slip on the Grand Valley fault. Royse and others (1975) showed this fault merging with the Absaroka thrust, but we believe that 4-km slip requires a more deeply rooted geometry. No major normal faults cut through the Snake River Range (Woodward, 1986) or the next range north, the Tetons (Love and others, 1992). Along the Teton fault, the hanging wall was vertically downfaulted 2.5 km since emplacement of the 2.0 Ma Huckleberry Ridge Tuff (HRT) and 5 km since a 5.5-Ma tuff was emplaced (Pierce and Morgan, 1992). We estimate 10 km of total offset, measured along the Teton fault from the projected hanging wall trace of the 5.5-Ma tuff to the projected footwall trace of the HRT. Jackson Hole is the east edge of the Basin and Range Province.

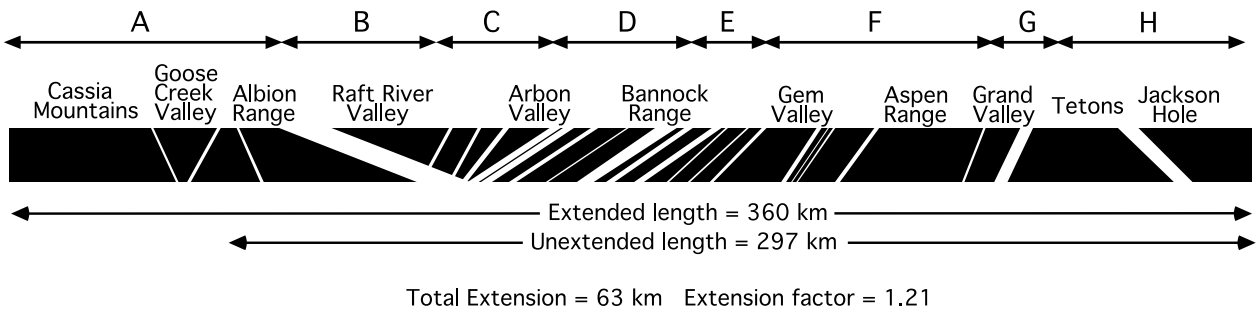

Figure 4. A schematic representation of the composite cross section shown in Figure 3 (and located in Figure 1), which summarizes fault geometry and kinematics. The slant and width of gaps reflect the dip and offset along Neogene-Quaternary normal faults.

Arbon Valley faults by Arbon Valley ramp), by inferred late Proterozoic rift-related faults, or by the west-thickening Paleozoic sedimentary sequence. Two major faults dip east. The Teton fault may have been controlled by the geometry of the underlying, east-dipping Cache Creek thrust fault (Lageson, 1992). What controlled the east dip of the Raft River detachment is unclear.

The spacing of normal faults is irregular. Faults are closely spaced in the central region, from Arbon Valley to the Aspen Range, and widely spaced from Jackson Hole to the Aspen Range and from Rockland Valley to the Cassia Mountains. Fault spacing appears to be inversely proportional to depth to crystalline basement, suggesting that deep-seated sedimentary rocks with subhorizontal weaknesses may have facilitated half-graben faulting. Alternatively, fault spacing may reflect proximity to the volcanic province to the north: Pierce and Morgan (1992) and Parsons and others (1998) noted that Basin and Range faults are more closely spaced near the SRP and suggested that they formed when the brittle-ductile transition was shallow because of an elevated geothermal gradient associated with magmatic activity.

The cumulative extension by middle Miocene to recent normal faults is about 63 km across a modern distance of 360 km, yielding 21 percent extension (Figure 4). Three faults account for half of the extension—the Raft River detachment (17 km from 17-7 Ma; Covington, 1983), the Fort Hall Canyon fault (7 km), and the Teton fault (7 km). Significant slip along each fault is also shown by the metamorphosed Archean or Late Proterozoic rocks in their footwalls (although in each place, uplift occurred in two phases). The most highly extended region is from Arbon Valley to Gem Valley, where numerous faults accommodated nearly 80 percent extension. As expected in a half-graben fault system, faults in this region dip more gently (25º-40º W.), and basin fill dips more steeply (25º-40º E.) than elsewhere. The region may be highly extended either because of its thick sedimentary sequence or because of reactivation of older thrust ramps or Proterozoic faults. Alternatively, the region may have experienced two magmatic events, each of which weakened the crust and allowed it to extend.

Basin and Range Faults North of the Eastern Snake River Plain

A continuous cross section through the entire Basin and Range just north of the eastern SRP has not been completed, but previous studies have estimated Basin and Range extension in the region. In east-central Idaho, three large normal faults, the Lost River, Lemhi, and Beaverhead faults, bound adjacent ranges (Figure 2). The faults generally strike northwest, dip southwest, and are bound on the southwest by sediment-filled basins as much as 3.5 km deep and on the northeast by ranges that rise as much as 2 km above the basins. The pattern of earthquakes as well as geodetic studies associated with the 1983 M_s = 7.3 Borah Peak earthquake on the Lost River fault clearly show it is a planar fault that dips about 50 degrees and extends to 16 km depth (Richins and others, 1987; Barrientos and others, 1987). All three faults are approximately 120 km in length. Janecke (1993) constructed balanced cross sections to measure 10-15 percent extension across east-central Idaho. Anders and others (1993) used tectonic tilts of fault blocks to measure 11 percent extension across southwestern Montana and east-central Idaho.

The typical Basin and Range landscape is absent to the west in central Idaho, replaced by highlands with few sedimentary basins. Across the White Knob and Pioneer Mountains, north- to northwest-striking, west-dipping normal faults are spaced 5-20 km apart and cut through fault blocks tilted 10º-25º E. (Rodgers and others, 1995). In the Smoky and Boulder Mountains (located 50 km north of the eastern SRP), Basin and Range faults have similarly broken the crust into gently northeast-tilted blocks (Rodgers and others, 1995) bounded by faults with relatively long continuous map traces. Major faults include the Sun Valley fault zone along the east side of the Wood River Valley, the Boulder fault along the front of the Boulder Mountains, and the Big Smoky fault along Big Smoky Creek. Offset along these faults was accompanied by 10-15 degrees of tilting to the northeast, as shown by regional outcrop patterns of subplanar volcanic and hypabyssal contacts (e.g., Mahoney, 1987) and sparse measurements of the attitudes of Eocene Challis Group volcaniclastic rocks. Overall, the typical east-northeastern tectonic tilt of 15 degrees indicates about 15 percent extension has been accommodated by Basin and Range faults.

In summary, two styles of Basin and Range faulting are evident north of the eastern SRP: widely spaced, segmented half-graben faults with significant offset and associated sedimentary basins and more closely spaced, relatively short half-graben faults with small offset and no associated basins. The contrast in style appears to correlate with a change in upper crustal rock type: Major faults to the east cut through a thick section of sedimentary rock, whereas minor faults to the west cut through the Eocene Challis volcanic field characterized by plutonic rock at shallow depths. Despite these differences, the cumulative extension throughout the region is consistently estimated at about 15 percent in a NE to ENE direction.

EXTENSION OF THE EASTERN SNAKE RIVER PLAIN

The absence of eastern SRP-parallel strike-slip faults, orographic bending, or minor pull-apart basins along the margins of the eastern SRP provide strong evidence that the eastern SRP experienced a kinematic history similar to that of the adjacent Basin and Range Province. Where individual faults can be traced from the Basin-Range into the eastern SRP, they progressively die out and overlap with volcanic rift zones (Quaternary faults) or are buried by younger rocks without showing evidence of diminished slip (Miocene-Pliocene faults). Because the Basin and Range experienced about 20 percent (south) to 15 percent (north) upper crustal extension, we interpret the crust of the eastern SRP to be similarly extended 15-20 percent in an ENE direction. Dikes and normal faults accommodated the extension in the upper crust, whereas the lower crust probably extended through dike injection and ductile attenuation. We predict that beneath the veneer of Quaternary basalt on the eastern SRP, the upper crust has structural relief and irregular topography reminiscent of the Basin and Range Province.

BASIN FILL: A RECORD OF EXTENSION AND MAGMATISM FROM 16 TO 0 MA

The stratigraphy of rock units in basins that flank the eastern SRP provides an excellent record of tectonism through time. Most basins formed as subsiding half grabens during active volcanism on the eastern SRP and thus contain a fairly complete stratigraphic record of both distal and proximal volcanic activity. The intercalated volcanic and sedimentary rocks, informally termed basin fill, are exposed today because of postdepositional tilting or deep incision by late Cenozoic streams, particularly along the southern margin of the eastern SRP where fault activity has ceased. We describe the evolution of two basins adjacent to the eastern SRP, one to the north and one to the south, to understand the initiation and duration of extension in the region.

Arbon Valley

Arbon Valley (Figure 2) is separated from the Bannock Range by the west-dipping Arbon Valley fault and from the Deep Creek Range by minor normal faults. Trimble and Carr (1976) defined the Neogene Starlight Formation in northern Arbon Valley where it consists of a lower member, a middle volcanic member (the tuff of Arbon Valley), and an upper member. Hladky and Kellogg (1987) remapped some of Arbon Valley prior to Bobo's (1991) detailed study of the Starlight Formation. Based on the latter work, we describe the stratigraphy and age of the Starlight Formation at two locations (Figure 5) and interpret depositional environments in the basin and their relation to eastern SRP tectonics.

The Trail Creek section, located in the northeastern corner of Arbon Valley, contains about 1,000 m of gently east-tilted Starlight Formation. The lower half includes a multitude of intercalated limestone and reworked tuffs. The limestones are interpreted to be lacustrine by lithology, primary sedimentary structures, and the type of fossils they contain. The intercalated tuffs indicate periods of silicic volcanism that inundated the lakes with voluminous pyroclastic material, temporarily exterminating the flora and fauna. New dating and correlation of ashes based upon their chemistry indicate an age range for these rocks from 15.65 Ma to older than 12.67 Ma (D.W. Rodgers, unpub. data). Basalt and 12.67-Ma rhyolite tuff are the next units upsection. Planar bedding and very fine ash laminae suggest emplacement of primary air-fall deposits into standing water. Paleocurrents indicate the flow or flows came from the southwest. The tuff is overlain by clast-supported conglomerate that is interpreted to be the channel deposits of a major meandering stream. Paleocurrent data indicate southeasterly flow, away from what is now the eastern SRP. Above the conglomerate is about 250 m of mostly loess-covered terrain containing rare outcrops of the 10.2 Ma tuff of Arbon Valley. The tuff of Arbon Valley heralds the beginning of massive, silicic volcanism that flooded much of Arbon Valley with deposits of pyroclastic flows and epiclastic tuffs. The number of exposures and the thicknesses of outcrops decrease to the south, ceasing altogether just south of Pauline, providing evidence of a source vent to the north. With the exception of an overlying 7.9-Ma porphyry lava, which occurs only in the extreme northern part of the valley, almost no basin fill is preserved above the tuff of Arbon Valley, indicating an end to deposition essentially after 10.2 Ma in this location.

The Pauline section of the Starlight Formation, located in central Arbon Valley, is dominantly siliciclastic. Drilling data indicate that bedrock is overlain by about 50 m of sandstone, which is overlain by about 10 m of exposed tuffaceous conglomerate intercalated with lenses of clay, sand, and tuff. This is overlain by two, nearly 100-m-thick sections of pebble-, cobble-, and boulder-conglomerate that locally fine upward. Pebble imbrications indicate a dominant northeast paleocurrent direction. The conglomerates are interpreted to be proximal and upper middle fan-facies fanglomerates with the coars-

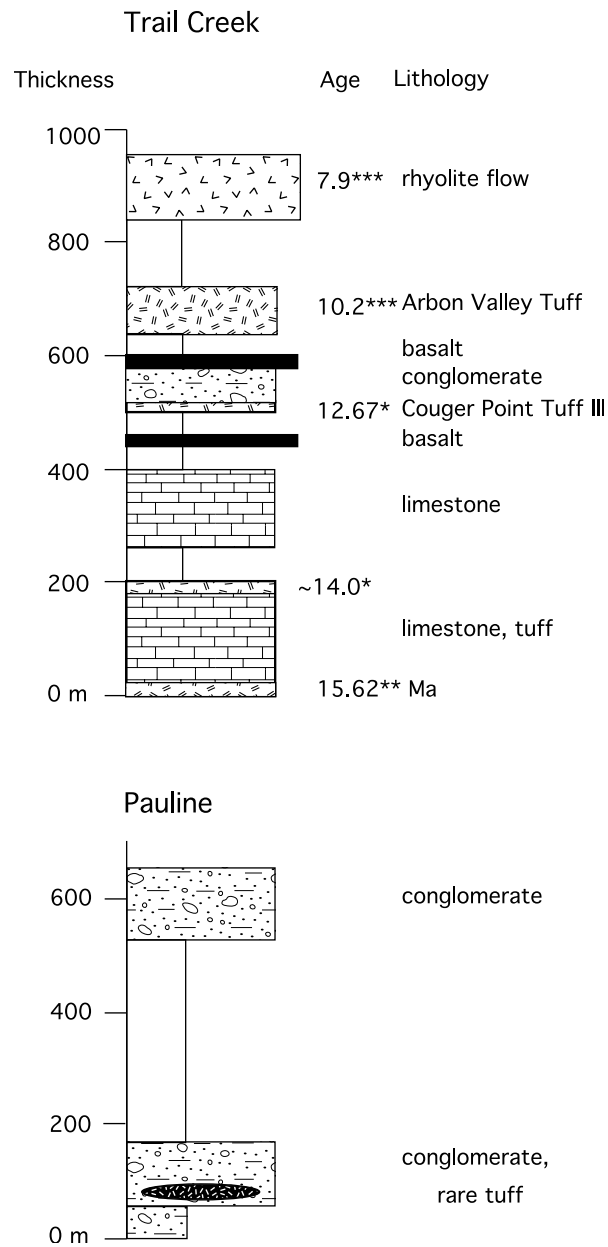

Figure 5. Stratigraphic columns of basin fill from Arbon Valley (modified from Bobo, 1991). Location of sections shown in Figure 2. Trail Creek section includes correlation ages (*) and $^{40}Ar/^{39}Ar$ ages (**) from David Rodgers (unpub. data), and $^{40}Ar/^{39}Ar$ ages (***) from Kellogg and others (1994).

est deposits representing channel lag deposits and the beds of pebbles, sand, and mud being sheetflood deposits. The tuff deposits and tuffaceous matrix testify to distant volcanic activity.

Thus, Arbon Valley evolved as a typical half graben: Erosion of horst blocks furnished siliciclastic sediments, and periodic eruptions from distant volcanoes provided significant quantities of silicic ash. Sediments were transported to the graben and produced rocks ranging from boulder conglomerates to fine mudstone in alluvial fan, fluvial flood-plain, and lacustrine environments. Trunk streams discharged into lakes that indicate a long-lived, poorly integrated, endorheic drainage system. In the northern part of the basin, proximal volcanism initiated with the emplacement of the 10.2-Ma tuff of Arbon Valley and 7.9-Ma lava flows. A second (or ongoing) pulse of faulting resulted in gentle to moderate half-graben tilting of the basin fill.

These results support the interpretation that Basin and Range faulting occurred before and during voluminous SRP magmatism in the region. From 16 to 10 Ma, when northern Arbon Valley subsided and filled, magmatism was focused to the west at the Owyhee Plateau and Twin Falls volcanic center. Syn- to post-10-Ma tilting of basin fill reflects extension that was approximately coeval with the eruption of the Arbon Valley tuff, the final 8.6-Ma volcanism in the Twin Falls volcanic center (Williams and others, 1990), or initial 6.5-Ma volcanism in the Heise volcanic field perhaps 50 km north of Arbon Valley (Morgan and others, 1984).

Southern Birch Creek Valley

Southern Birch Creek Valley (Figure 2) is bounded on the east by the Blue Dome segment of the west-dipping Beaverhead normal fault. Rodgers and Anders (1990) interpreted the stratigraphy and evolution of basin fill in the Lone Pine vicinity and in places throughout southern Birch Creek Valley. McBroome (1981), Kuntz and others (1984; 1994a), Rodgers and Zentner (1988), and Hodges and Rodgers (1999) described the stratigraphy of Howe Point at the southern end of Birch Creek Valley. Rodgers and Anders (1990) suggested a northward migration of both fault initiation and cessation for southern Birch Creek Valley. In this paper, we focus on fault initiation and its timing relative to proximal eruption of rhyolite volcanic rocks.

Angular unconformities and disconformities separate all units exposed at Howe Point (Figure 6). The Medicine Lodge beds, which include 90 m of fanglomerate with minor lacustrine limestone and volcanic ash, accumulated about 16.1 Ma as determined by the age of intercalated volcanic ash near the top of the sequence. Though no syn-depositional fault was observed, these rocks are typical of half-graben basin fill and thus interpreted to reflect the earliest Basin and Range tectonism in the region. Attitudes of these and overlying rocks provide evidence of 23 degrees of south-southeastward tilting between 16-10 Ma, followed by 52 degrees of east-northeastward tilting between 10-0 Ma (Figure 7). These two tilt directions are most simply interpreted as an early pulse of flexure associated with eastern SRP subsidence (described below) and as progressive tilting associated with ongoing Basin and Range tectonics. Furthermore, all rocks older than 6.0 Ma are very gently folded about an ENE-trending axis, which McQuarrie and Rodgers (1998) interpreted in terms of a late, minor (12 degrees) pulse of subsidence-related flexure.

In contrast, Neogene rock units near Lone Pine are more commonly separated by disconformities (Figure 8), suggesting no significant tilting of the Neogene section until after Pliocene-Pliestocene conglomerate deposition (Rodgers and Anders, 1990). Despite fewer angular unconformities, the existence of a fault-bounded basin during Medicine Lodge accumulation is supported by the presence of conglomerate east and west of correlative limestone and by the eastward shift in depocenters from the Medicine Lodge beds basin to the Lone Pine basalt basin. Faulting just before the accumulation of Lone Pine basalt is strongly supported by the map pattern and basalt thickness, indicating the basalt filled an asymmetric valley with stream channels projecting into the Lemhi Range. Significant tilting, and by inference faulting along the Beaverhead fault, did not begin at Lone Pine until after deposition of Pliocene-Pliestocene conglomerate.

These data clearly show a northward decrease in the initial age and amount of extensional displacement, a pattern interpreted by Rodgers and Anders (1990) to reflect the outward migration of a Neogene seismic parabola.

TIMING OF REGIONAL EXTENSION

Stipulating that many Basin and Range faults project onto the eastern SRP and that the eastern SRP and adjacent Basin and Range Province share a common kinematic history, the age or ages of extension in the two provinces should be similar. Thus, the timing of Basin and Range normal faulting can be used to indicate the timing of eastern SRP extension.

In addition to detailed analysis of associated basin fill, such as described above for Arbon Valley and Birch Creek Valley, the age of normal faulting can be determined by cross-cutting relations between faults and datable rocks, by thermochronologic studies of uplifted fault blocks, and (for active terrains) by the study of fault scarps

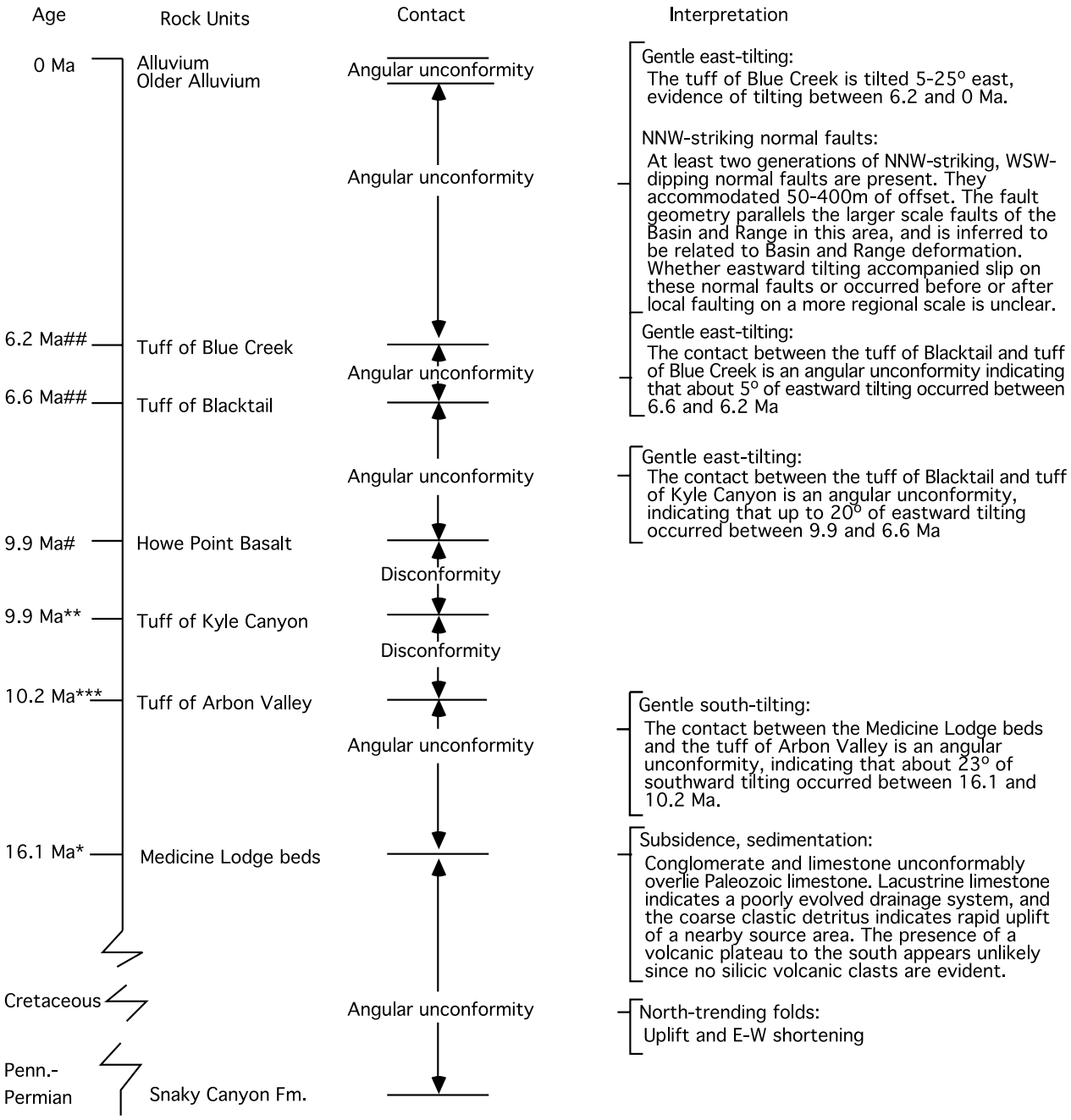

Figure 6. Summary of deformation and basin filling at Howe Point in southernmost Birch Creek Valley. See Figure 2 for location of Howe Point. Sources of radiometric ages: (*) from Anders (unpublished), (**) from Morgan and others (1984), (***) Kellogg and others (1994), and (##) from Rodgers and Anders (1990). Figure modified from Rodgers and Zentner (1988).

and geomorphic features. Unfortunately, cross-cutting relations are rarely exposed, and no late Cenozoic fission-track or $^{40}Ar/^{39}Ar$ ages have been reported from uplifted footwalls for the region, apparently because of insufficient uplift or difficulty in obtaining adequate samples. To interpret the ages of normal faulting across the region, we summarize the ages and texture of basin fill along the southern margin of the eastern SRP. In concert with existing neotectonic data, such as the relative degrees of Quaternary fault activity (Turko and Knuepfer, 1991; Pierce and Morgan, 1992) and the ages of recent individual fault events based on trenching, these data indicate the space-time pattern of extension that we interpret to have affected the eastern SRP.

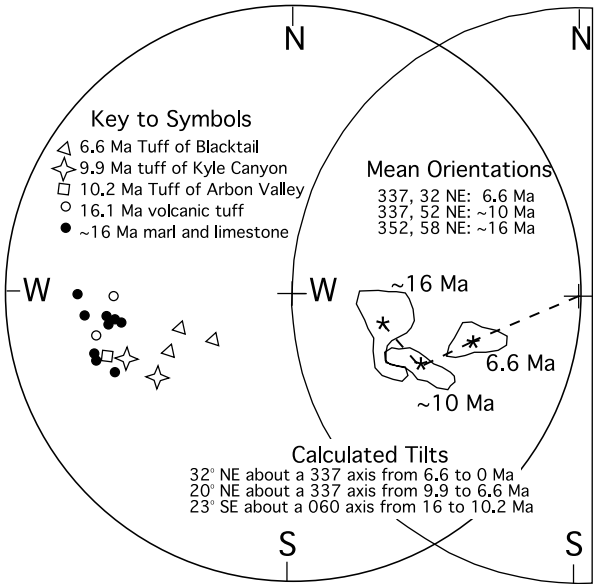

Figure 7. Lower hemisphere, equal area projection of poles to bedding and compaction foliation in Miocene rocks at Howe Point, southernmost Birch Creek Valley. Left figure shows measured orientations of rocks. Right figure shows mean orientations of rocks in three age groups. The calculated tilts would generate the angular unconformities between groups. These data provide evidence of eastern SRP flexure from 16-10 Ma and Basin and Range tilting from 10-0 Ma.

Figure 9 summarizes the interpreted age span of extension in several localities across southern Idaho and adjacent regions. The figure assumes that basin filling was associated with extensional faulting. The figure also presents an incomplete record of extension because the lower basin fill in several localities is undated. The figure does not indicate north-to-south variations in extensional age or extensional pulses unaccompanied by basin filling. Although more field-based study of extensional tectonics is needed throughout the region to clarify the detailed pattern of extension, Figure 9 shows a regional pattern first recognized by Allmendinger (1982) that we interpret as two periods of Neogene extension.

First, the entire region extended in the middle Miocene. Basins in southern Idaho generally contain less than 1,000 m of volcanic and fine-grained sedimentary rocks, evidence of only minor extension at this time in contrast to northern Nevada where signficant extension is indicated by basins with more than 3,000 m of basin fill. Basin filling began as early as 15.7 Ma in Arbon Valley and before 10.2 Ma in Buckskin Basin, Swan Valley, and Jackson Hole. Basin filling ceased by about 12 Ma in Arbon Valley and 9 Ma in Jackson Hole, but slow subsidence continued in other regions (Figure 9).

A second period of extension affected southern Idaho and western Wyoming during the last 9 million years, as manifested by the accumulation of thick, coarse-grained basin fill or the rapid tilting of basin fill (Figure 9). We infer that most of the extension across southern Idaho and western Wyoming occurred during this second pulse of extension. Both the beginning and end of this extensional pulse becomes younger from west to east, evidence that an east-migrating pulse of major extension passed across southern Idaho. The modern coincidence of this pulse with the Quaternary fault zones of Pierce and Morgan (1992) and the seismic parabola of Anders and others (1989) is strong evidence that the same pattern and migration of normal faults existed during the late Neogene.

CRUSTAL SUBSIDENCE

Although high in regional elevation, the eastern SRP is a topographic and structural depression (Figure 1). Along its axis, the surface slopes gently southwest from an elevation of about 3 km on the Yellowstone Plateau to 1.5 km near Twin Falls. Across its axis, the surface is relatively flat, with a subtle axial highland. At its margins, the terrain rises from elevations of 1.5-2 km on the lava plains to 2-4 km in the valleys and mountains of the Basin and Range. Two wavelengths of cross-axis topography are evident: a short wavelength depression about 40 km wider than the eastern SRP, and a long wavelength depression about 150 km wider than the eastern SRP. Short wavelength, cross-axis structural relief is manifested by marginal Paleozoic and Miocene rocks that dip gently toward the eastern SRP.

Kirkham (1927, 1931) first recognized and described the “Snake River downwarp” by noting a number of geomorphic features and some tilted rocks that consistently dipped toward the eastern SRP. Suppe and others (1975) insightfully described regional topography and emphasized the downwarp’s relation to hot-spot magmatism. Surface subsidence along the axis of the eastern SRP that increased as a function of distance from the Yellowstone Plateau was documented by Reilinger and others (1977) and modeled as thermal contraction (Brott and others, 1981; Blackwell and others, 1992) or as a relative increase in loading by dense magmatic intrusions (Anders and Sleep, 1992). Indeed, it is the gradual northeast to southwest decrease in eastern SRP elevation that supports the theory that the eastern SRP marks the passage of western North America over a mantle plume.

Because vertical motions of the crust are intricately tied to other tectonic processes, the subsidence history of the eastern SRP is an important record of events otherwise obscured by younger events and rocks. Subsidence

data can be obtained from several eastern SRP sources, including drill holes, topography, seismic, and gravity studies, or from analysis of the eastern SRP margins where faults, tilted rocks, and angular unconformities are present. Many other workers have described and interpreted the eastern SRP data (Reilinger and others, 1977; Doherty and others, 1979; Pankratz and Ackermann, 1982; Greensfelder, 1981; Sparlin and others, 1982; Blackwell and others, 1992; Anders and Sleep, 1992; Saltzer and Humphreys, 1997; Peng and Humphreys, 1998), but few have focused on subsidence recorded along the eastern SRP margins. In the following sections, we describe the

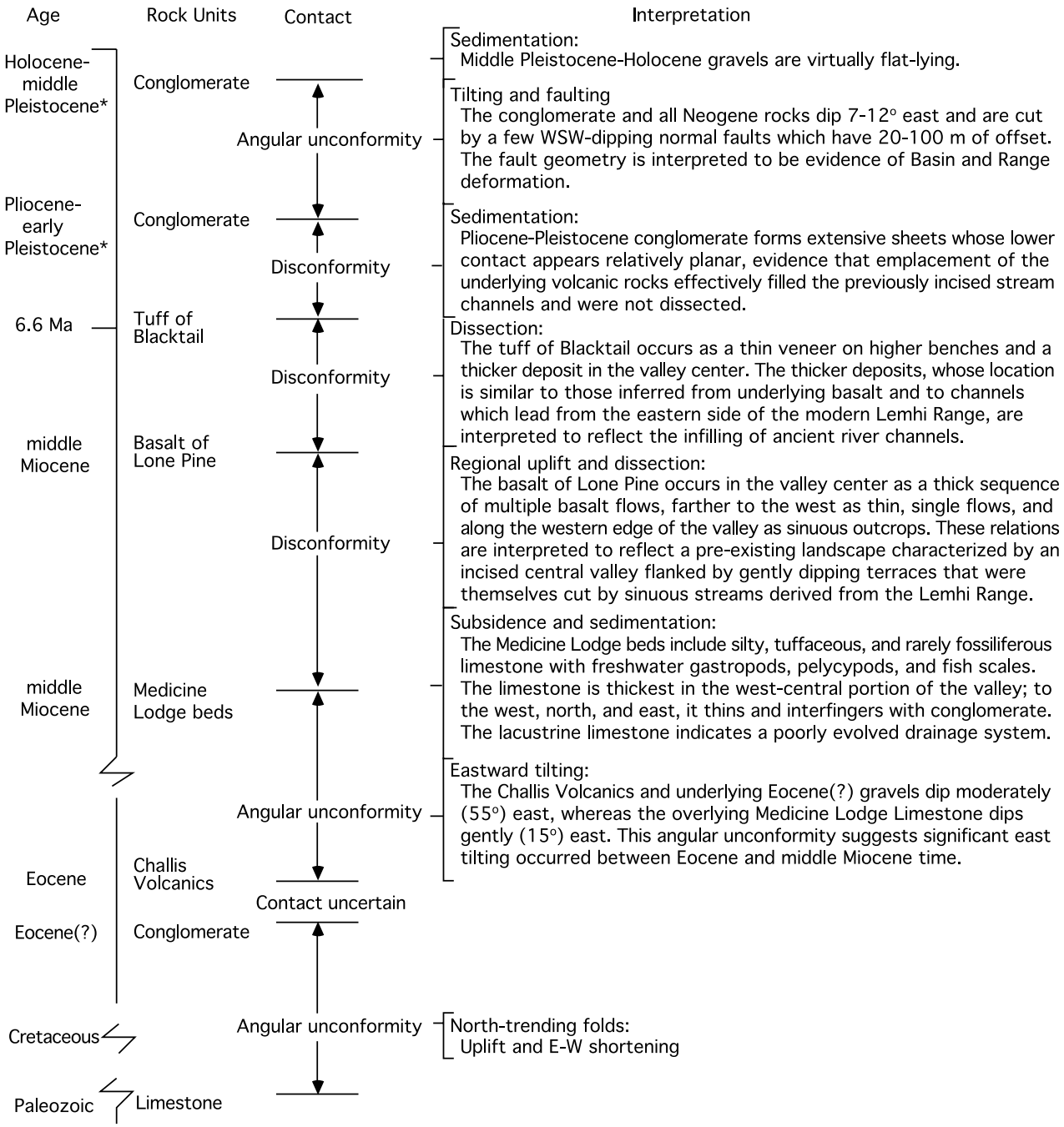

Figure 8. Summary of deformation and basin filling at Lone Pine in southern Birch Creek Valley. See Figure 2 for location of Lone Pine. Ages (*) from Scott (1982).

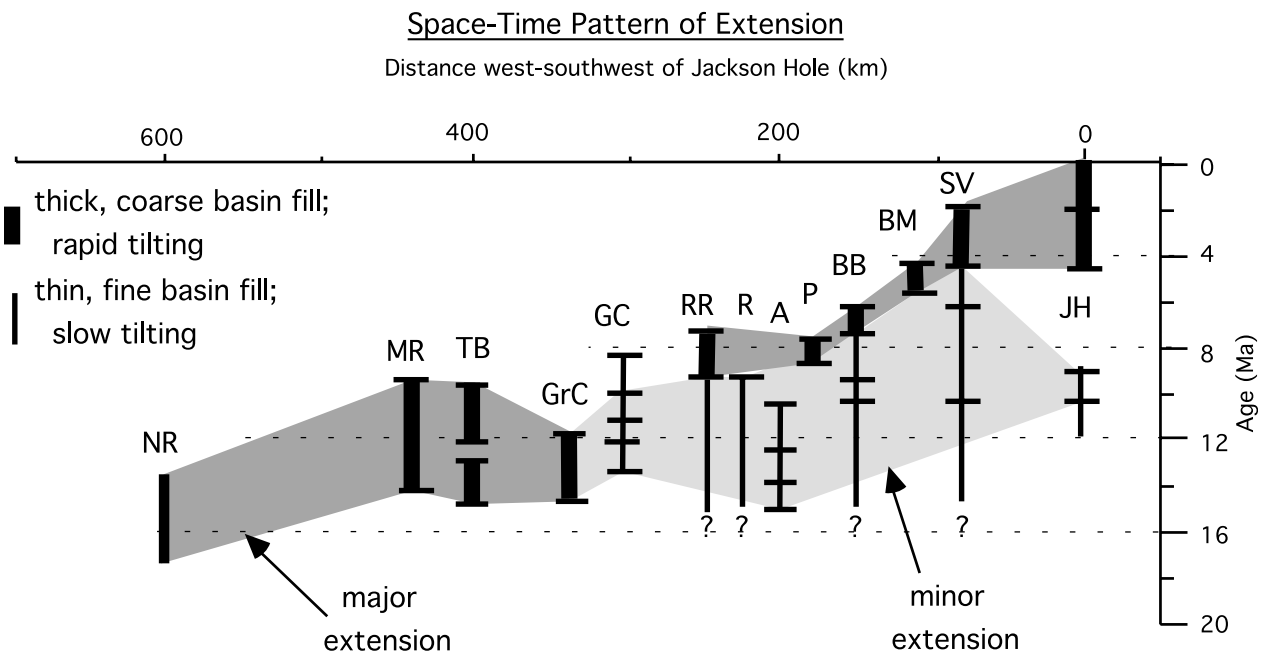

Figure 9. Interpreted age span of extension in specific localities across southern Idaho and adjacent Nevada and Wyoming. Horizontal bars indicate dated volcanic rocks. Extension manifested by dike injection (NR), relative rates of basin-fill tilting (SV), normal faults cut by volcanic rocks (BM), and the age span of basin fill (all other localities). Dark shading indicates a pulse of major extension and light shading a pulse of minor extension. Localities and sources of data include northern Nevada rift (NR; Zoback and Thompson, 1978), Mary's River (MR; Mueller and Snoke, 1993), Toano basin (TB; Mueller and Snoke, 1993), Grouse Creek Valley (GrC; Compton, 1983), Goose Creek Valley (GC; Perkins and others, 1995), Raft River Valley (RR; Williams and others, 1982), Rockland Valley (R; Trimble and Carr, 1976; this paper), Arbon Valley (A; Bobo, 1991; this paper), Portneuf Valley (P; this paper), Buckskin Basin (BB; Kellogg and Marvin, 1988), Blackfoot Mountains (BM; Allmendinger, 1982), Swan Valley (SV; Anders and others, 1989; Anders, 1990), and Jackson Hole (JH; Love, 1977; Love and others, 1992; Pierce and Morgan, 1992; Perkins and Nash, 1994). Figure modified from Rodgers and others (1990, 1994).

results of several studies undertaken to document the style, geometry, and timing of eastern SRP subsidence. These data, in conjunction with previous studies of the eastern SRP itself, provide a new view of crustal processes associated with magmatism and deformation.

Two types of eastern SRP subsidence will be discussed. Both are measured relative to rocks and elevations of the adjacent Basin and Range Province, not to an external reference plane such as sea level (England and Molnar, 1990). One type is rock subsidence, characterized by a decrease in vertical position. Where rock subsidence is accommodated via structural tilting we use the term crustal flexure. The other type is surface subsidence, characterized by a reduced elevation of the earth's surface. Where surface subsidence is manifested by regional topographic gradients, we use the term downwarping.

NORMAL FAULTING

Based on seismic velocity data from the 1978 Yellowstone-eastern SRP seismic experiment, Sparlin and others (1982), Braile and others (1982), and Smith and others (1982) suggested that the eastern SRP experienced subsidence by downdropping, half-graben style, along a normal fault at its northern margin. If the fault exists, it is concealed beneath the Quaternary basalts of the eastern SRP and thus unavailable for structural analysis. However, other northeast-striking normal faults are present just beyond the eastern SRP in the Basin and Range. To document fault style and geometry, Zentner (1989) mapped normal faults in the southern Beaverhead Range (Figure 2) where they offset Neogene ash-flow tuff whose distinct lithologies, instantaneous emplacement, and widespread lateral extent make them ideal for study. Zentner (1989) also used published maps adjacent to the entire eastern SRP to determine the lateral extent of similar faults. More recently, Kellogg (1990) and Rodgers and Othberg (1999) have mapped similar faults in the northern Portneuf and Bannock Ranges (Figure 2). The results of these studies are reported below.

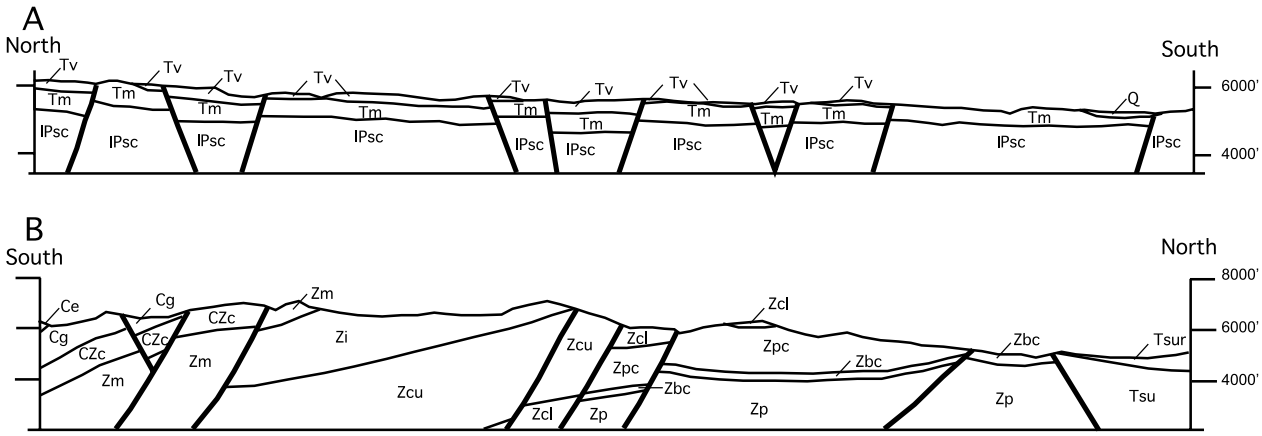

Figure 10. Cross sections showing fault patterns adjacent to the eastern SRP. A is north to south cross section near Lidy Hot Spring (located in Figure 2). B is south to north cross section in the northern Bannock Range (located in Figure 2). After Zentner (1989) and Rodgers and Othberg (1999).

Lidy Hot Springs, Southern Beaverhead Range

The Lidy Hot Springs area at the southern tip of the Beaverhead Mountains (Figure 2) contains a sequence of sedimentary rocks and ash-flow tuffs (Embree and others, 1982). Two distinct normal fault sets are apparent in the study area, a northwest-striking set and a northeast-striking set. The faults cut all rock units of the area, except the Quaternary gravel, and truncate each other at various locations throughout the field area.

The NNW-striking normal fault set comprises a series of faults spaced 0.1 to 0.7 km apart. No fault surfaces are exposed, but fault traces are located where formations are juxtaposed contrary to their depositional order. Strikes of faults in this set average N. 25º W.; their dips range from 55-65 degrees both northeast and southwest. Individual faults offset the ash-flow sheets as much as 250 m. Calculations of the area's width before and after extension show that the area was extended about 7 percent northeast-southwest by these faults. The age of the fault set is between the age of the youngest unit offset by faults (4.3-Ma tuff of Kilgore) and the age of the oldest unit (Quaternary alluvium) not offset. Because the normal faults are parallel to major Basin and Range normal faults in the region, they are interpreted to reflect Basin and Range extension.

The ENE-striking normal fault set (Figure 10) comprises faults that are spaced 0.3 to 0.7 km apart and generally extend several kilometers in length. They show no evidence of strike-slip movement, which discredits ideas that the eastern SRP represents a major strike-slip zone between regions of differential extension (Pratt, 1982). Strikes of the faults in this set average around N. 60º E., and their dips are 70-80 degrees both northwest and southeast. Individual faults offset the ash-flow tuffs up to 100 m. Calculations of the area's width before and after extension show that the area was extended only 2 percent northwest-southeast. Cross-cutting relations with rocks and the NNW-striking fault set indicate that both fault sets were active at the same time.

Northern Bannock Range

Northeast-striking normal faults were mapped in detail in the northern Bannock Range (Figure 2) by Rodgers and Othberg (1999) and in the northern Portneuf Range (Figure 2) by Kellogg (1990). Here, normal faults cut Proterozoic to Middle Cambrian strata that previously experienced both Cretaceous shortening and Basin and Range extension. The eastern SRP-parallel faults strike east-northeast to northeast, are spaced 1-5 km apart, dip moderately to steeply southeast, and typically show 100-1,000 m of normal slip (Figure 10). The cumulative result of fault offset is to uplift rocks in the north more than rocks in the south. The Bannock Range faults postdate regional tilting associated with 9-7.3 Ma basin formation, show a mutually cross-cutting relation with the range-bounding fault, and do not cut across 0.6 Ma basalt.

Normal Faults Along the Margins of the Eastern Snake River Plain

To document the regional extent and pattern of northeast-striking normal faults along the margins of the eastern SRP, Zentner (1989) compiled published geologic maps of areas within 50 km of it. As shown in Figure 11,

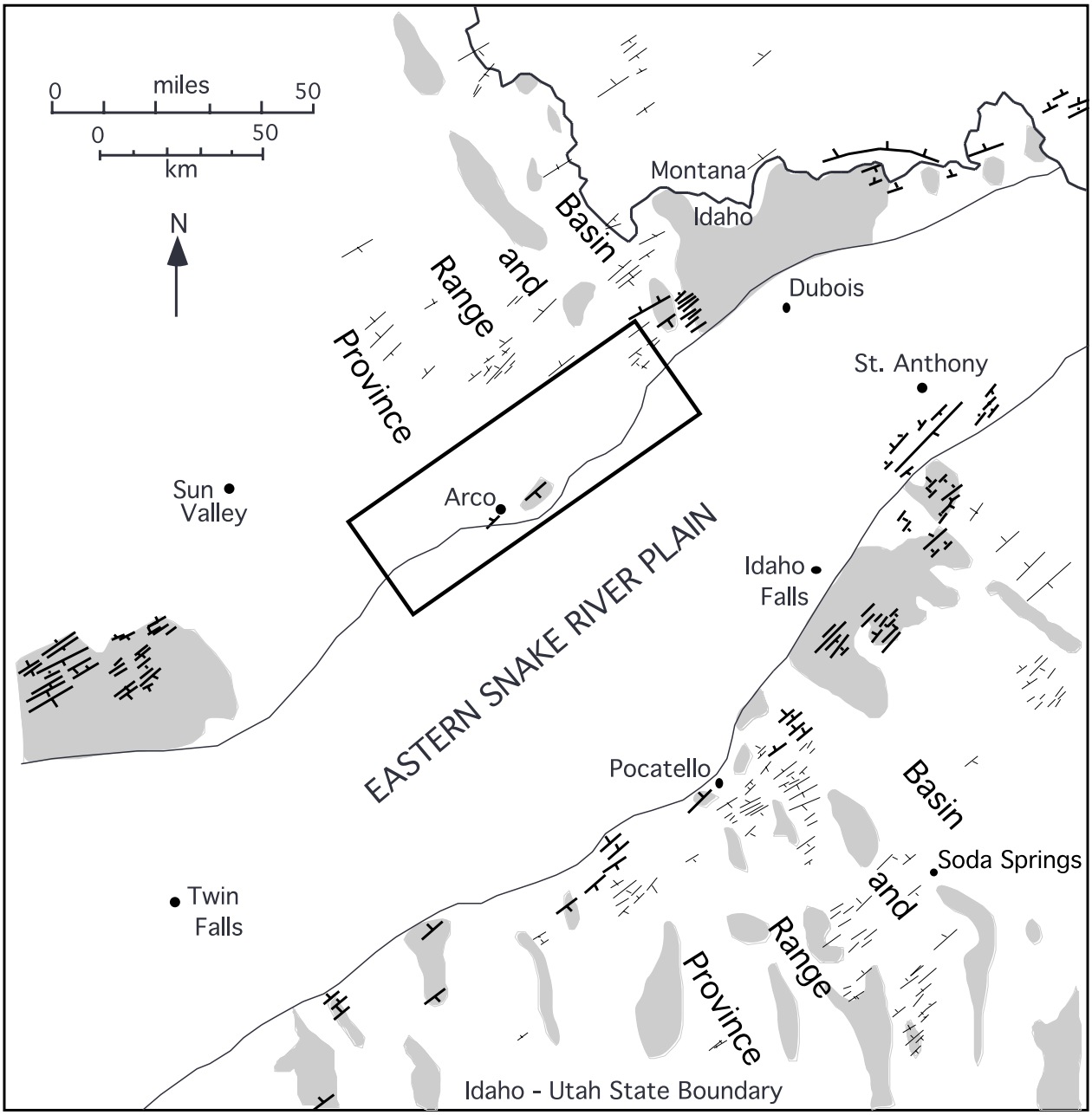

Figure 11. Compilation of northeast-striking normal faults adjacent to the eastern SRP from Zentner (1989). Faults that cut rocks older than 10 Ma are represented by thin lines, whereas faults that cut 10 Ma and younger rocks are indicated by thick lines. Distribution of Tertiary rocks younger than 10 Ma is shaded. Northeast-striking faults younger than 10 Ma are restricted to a 30-km zone adjacent to the eastern SRP. Rectangle is location of Figure 12. Sources of data include Albee and Cullins (1965), Armstrong and others (1978), Burgel (1986), Carlson (1968), Cluer and Cluer (1986), Corbett (1978), Cress (1981), Garmezy (1981), Hladky (1986), Kellogg (1990), Kellogg and others (1989), LeFebre (1984), Oriel (1980), Oriel and Moore (1985), Pierce and others (1983), Schmidt (1962), Skipp (1988), Skipp and others (1990, 1992), Trimble (1980), Trimble and Carr (1976), Waldrop (1975), Witkind (1972, 1976).

northeast-striking faults are present throughout southern Idaho, western Wyoming, and southwestern Montana and are both adjacent to and distant from the eastern SRP.

Because southern Idaho has experienced a protracted deformational history, northeast-striking faults in the region may have formed during Mesozoic thrusting, Neogene Basin and Range faulting, or Neogene development of the eastern SRP. To discriminate faults of different ages, northeast-striking faults that cut rocks younger than about 10 Ma are distinguished from faults that cut rocks older than 10 Ma (Figure 11). The ages of faults in pre-10 Ma rocks are uncertain: they may also be younger than 10 Ma, or they may be older than 10 Ma and therefore unrelated to the eastern SRP.

Figure 11 shows that northeast-striking faults younger than 10 Ma are restricted to two zones, each about 30 km wide, along the northern and southern margins of the eastern SRP. Tertiary rocks not cut by northeast-striking faults are more than 30 km from the eastern SRP margins, indicating that the zones of faults are situated near the margins of the eastern SRP. Because of their orientation, their proximity to the eastern SRP, and their similar age to the eastern SRP, these faults are inferred to be related to the development of the eastern SRP. Although the kinematics of these faults are in most places unknown, where they have been studied (Allmendinger, 1982; Smith, 1966; Hladky, 1986; Pogue, 1984) the faults show normal dip-slip displacements of less than 1 km. Thus, their style and geometry appear to be identical to the northeast-striking faults of the Lidy Hot Springs, Portneuf, and Bannock regions.

The age of the northeast-striking normal faults across the region is poorly constrained. Zentner (1989) and Allmendinger (1982) determined the age of faulting to be between 4.7 Ma and about 2.0 Ma, and Rodgers and Othberg (1999) bracketed the age of faults between 7.3 and about 0.6 Ma.

Interpretation of Northeast-Striking Normal Faults

Before this study, it was assumed that since the plain is a structural basin, the northeast-striking normal faults must have accommodated the downdropping of the plain (Sparlin and others, 1982). Certainly the structural parallelism of the northeast-striking normal faults and the axis of the eastern SRP, as well as the coeval development of the faults and eastern SRP, support the interpretation that the faults and eastern SRP are genetically related. Zentner's (1989) mapping, however, shows that the net vertical displacement along these normal faults is minimal, and many of the faults dip away from the eastern SRP's axis. Thus, the exposed northeast-striking normal faults clearly do not contribute to a structural downdropping towards the plain. Alternate interpretations of plain-parallel normal faults include (1) regional northwest-southeast extension, (2) faulting along caldera margins, (3) horizontal thermal contraction, and (4) extension related to crustal flexure. We believe the first three options are not supported by the distribution, geometry, and kinematics of faulting. However, the zone of normal faults is coincident with a zone of downwarping first described by Kirkham (1927, 1931). Recognizing the coincidence of faults and downwarped crust, Zentner (1989) proposed that the minor northeast-striking normal faults along both margins of the eastern SRP formed as the rigid uppermost crust flexed downward beneath the eastern SRP. As observed in foreland basins and subducting oceanic slabs (Turcotte and Schubert, 1982), such flexure would be accompanied by extensional structures of uniform orientation, restricted extent, and variable dips identical to the faults observed in this study. This interpretation is most consistent with the available data and is strongly supported by the more recent work of McQuarrie (1997; and summarized below), who measured the extent and amount of crustal flexure and confirmed that it was coincident with the zone of northeast-striking normal faults. Thus, the normal faults along the margins of the eastern SRP are interpreted to reflect extension due to crustal flexure.

ROCK SUBSIDENCE AND CRUSTAL FLEXURE

Subsidence of the eastern SRP and the associated downwarping and flexure of the adjacent Basin and Range are manifested by surface tilts and 1- to 20-degree structural dips of late Cenozoic rocks toward the eastern SRP (Kirkham, 1927, 1931; Trimble and Carr, 1976; Rodgers and Anders, 1990; Houser, 1992). To systematically measure the amount and distribution of crustal flexure and to interpret the mechanisms of eastern SRP crustal subsidence, McQuarrie (1997; and McQuarrie and Rodgers, 1998) completed a quantitative analysis of crustal flexure along the northwestern margin of the eastern SRP.

Crustal Flexure

Crustal flexure adjacent to the eastern SRP should cause Cretaceous fold hinges in Paleozoic rocks to tilt toward the plain. If these fold hinges were originally horizontal, the amount of flexure can be determined. McQuarrie (1997) measured the plunges of 313 Cretaceous fold hinges, and locally the dip of Neogene vol-

canic rocks, to quantify the amount of flexure. Fold data indicate a regular pattern of orientations: fold hinges trend southeast approximately perpendicular to the trend of the eastern SRP, plunge 0º-25º SE., and show a progressively increasing plunge to the southeast. After accounting for tilting due to Basin and Range extension, the fold data were contoured to smooth out irregularities, emphasize overall trends, and provide numerical values for areas with no measured folds. The map of contoured fold hinges shows a consistent pattern throughout the study area (Figure 12). The contour lines parallel the axis of the eastern SRP and define a narrow downwarped zone that extends approximately 10-20 km north of the eastern SRP. They also show a southeastward increase in plunge, to a maximum of 25º SE. A second-order trend is the prominent pattern of reentrants and salients that give a scalloped appearance to the contours. The reentrants make sharp curves inward on both the ranges (Pioneer Mountains and the Appendicitis Hills) and the intervening valleys (Little Lost River Valley and Birch Creek Valley) and have both closely and widely spaced contours (Figure 12).

Cross sections show that measured structural relief due to flexure is much greater than the 1.5 km indicated by topographic relief and that the structural surface de-

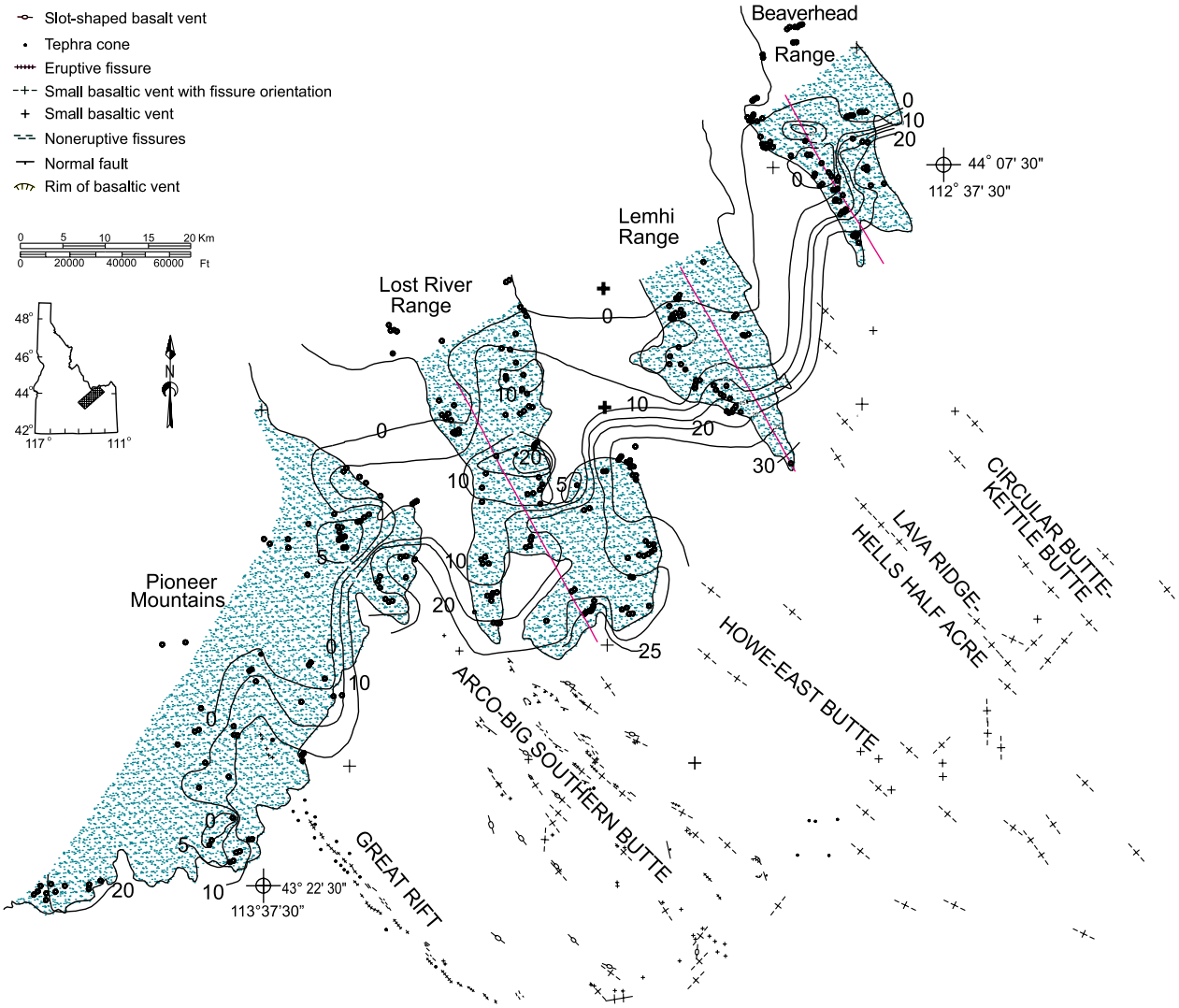

Figure 12. Summary of crustal flexure along the northern margin of the eastern SRP. Black dots in the ranges are locations where Cretaceous fold plunges were measured. Contours represent lines of equal southward fold plunge through the study area. The contour interval is 5º. Fold plunges increase from 0º to greater than 20º to the south. Also shown are Quaternary volcanic rift zones on the eastern SRP (after Kuntz and others, 1992), which emphasize their spatial correlation to reentrant contours. Location of figure is shown in Figure 11. Modified from McQuarrie (1997).

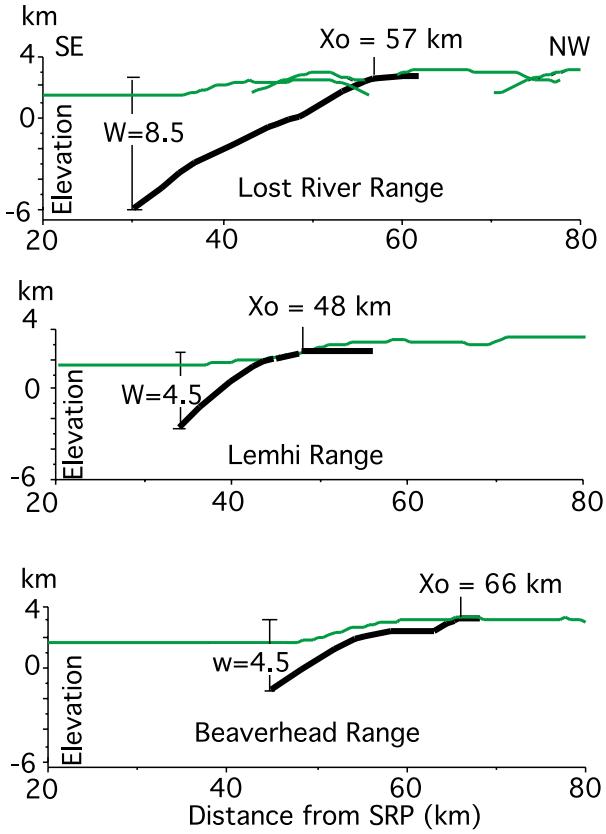

Figure 13. Cross sections of crustal flexure and topography along the northern margin of the eastern SRP. Topographic downwarping is shown by thin lines that are average elevations of ranges measured along each ridge crest. Crustal flexure is shown by bold lines that represent the projected plunge of folds measured along the surface. W = minimum amount of measured crustal flexure. X_0 is half-width of eastern SRP, measured from 0º plunge to eastern SRP axis. Sections are located in Figure 12. Figure from McQuarrie (1997).

lineated by plunge values does not parallel topography (Figure 13). Structural relief ranges from 4.5 to 8.5 km, amounts which represent the minimum rock subsidence of the eastern SRP with respect to the Basin and Range.

Crustal flexure has not been systematically examined beyond the study area of McQuarrie (1997), although such work is currently underway. The ubiquitous development of topographic downwarping along the eastern SRP margins is a good indication that crustal flexure everywhere flanks the eastern SRP and is supported by measurements of tilted structural markers elsewhere (Trimble and Carr, 1976; Houser, 1992; Rodgers, unpubl. data, 1995).

Eastern Snake River Plain Loading Mechanisms

The pattern of subsidence and downwarping reveals that a laterally extensive, crustal to lithospheric process has affected the greater eastern SRP region. McQuarrie (1997) and McQuarrie and Rodgers (1998) attributed regional subsidence of both rocks and the surface to the isostatic compensation of a load emplaced on or beneath the eastern SRP; the load is imposed by crustal layers that are thicker or denser than correlative layers in the adjacent Basin and Range. Loading by thermal contraction of the eastern SRP was rejected because heat flow is greater on the eastern SRP (107 mWm^{-2}) than on the adjacent Basin and Range (80 mWm^{-2}; Blackwell and others, 1992). Loading by the 5- to 8-km-thick sequence of basalts and underlying sediments and rhyolites, which constitute the "basin fill" of the eastern SRP, was also rejected because these rocks have relatively low densities (2.5 g cm^{-3} according to Sparlin and others, 1982). Loading generated by dense mafic rock that was emplaced into the eastern SRP crust is the preferred mechanism, and previous work suggests that such rocks are present at depth (Leeman, 1982; Sparlin and others, 1982; Greensfelder, 1981; Anders and Sleep, 1992).

Flexural Modeling

Flexural modeling was used to test the hypothesis that a dense crustal layer or layers beneath the eastern SRP could generate the appropriate load to produce the observed downwarping and flexure along the eastern SRP flanks and to provide a range of load dimensions that could produce the measured flexure as well as estimates of crustal strength and depth of compensation. A flexure model developed for the study of an aulocogen (Nunn and Aires, 1988) was applied to eastern SRP subsidence, with the exception that no extension was included. As reported in McQuarrie and Rodgers (1998) and shown in Figure 14, the main results of modeling include the following:

(1) Subsidence was isostatically compensated in the lower crust, not asthenosphere, because only crustal compensation allows for the development of a relatively narrow, deep basin like the eastern SRP. Compensation in the lower crust is supported by a flat Moho (Sparlin and others, 1982; Peng and Humphreys, 1998), by a close relationship between topography and Bouguer gravity suggesting compensation by plastic flow within the upper 20 km of the crust (Eaton and others, 1978), and by a high heat flow sufficient for partial melting or subsolidus grain-boundary relaxation of the lower crust (Greensfelder, 1981; Blackwell and others, 1992).

(2) The calculated strength of the Basin and Range crust is very low, as expected with such a high heat flow. Flexural parameters of 5-10 km are slightly lower than

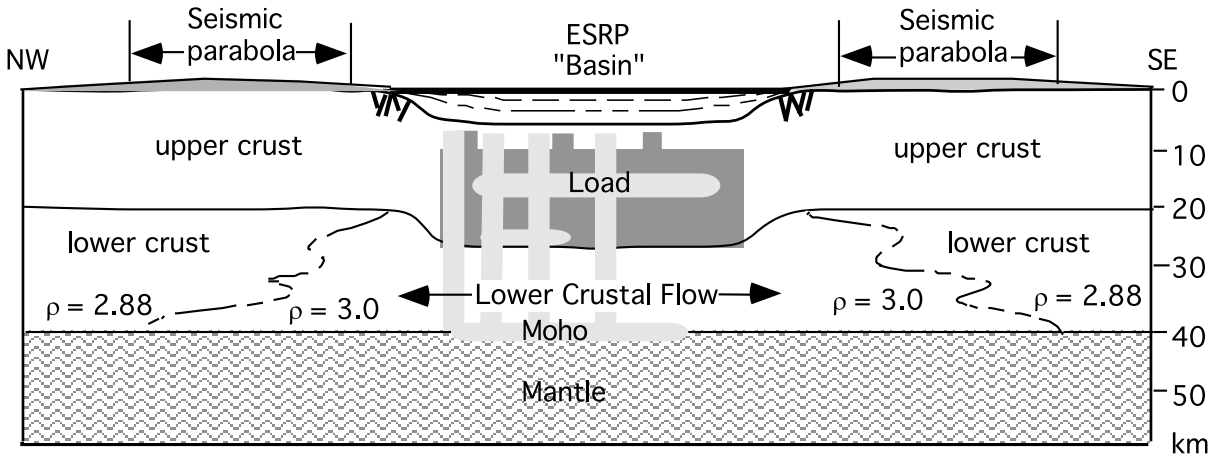

Figure 14. Summary figure depicting crustal flexure and subsidence associated with the eastern SRP. Figure shows (1) an extensive midcrustal load emplaced by 10 Ma (black area), (2) a post-Neogene load related to the volcanic rift zones (gray area), (3) 5-8 km of downwarped Basin and Range crust, (4) a northeast-striking fault set associated with flexure of the crust (Zentner, 1989), (5) an angular unconformity between the downwarped fold hinges and volcanic rocks of the SRP (dashed lines), (6) a flat Moho, and (7) lower crustal flow from beneath the eastern SRP to the extending Basin and Range (seismic parabola). Figure from McQuarrie and Rodgers (1998).

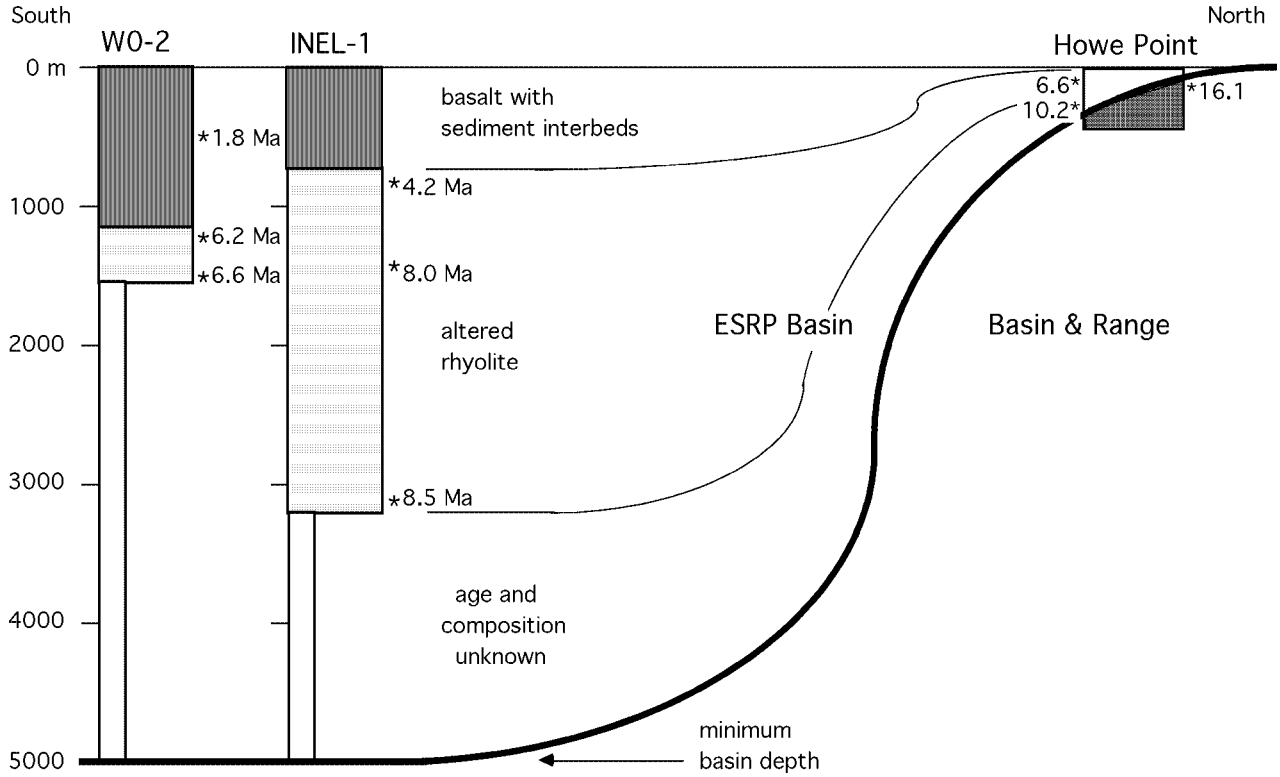

Figure 15. Schematic cross section along the northern margin of the eastern SRP showing age-depth relations of various horizons and rock units. See text for discussion. Data from Morgan and others (1984), Anderson and others (1997), McQuarrie and Rodgers (1998), and M. McCurry (oral commun., 1999).

previous estimates of about 12 km (Anders and others, 1993; Lowry and Smith, 1995), and much lower than that typical of cratonal regions.

(3) The eastern SRP crustal layering proposed by Sparlin and others (1982) would induce somewhat less subsidence and a wider depression than is actually observed. To produce a close match between model and actual flexure curves, a middle crustal sill must have a half width of 40-50 km, roughly coincident with the borders of the eastern SRP, and a thickness ranging from 17 to 25 km if its average density is 2.88 g cm^{-3}.

Age and Rate of Rock Subsidence

The age of initial rock subsidence is unknown because the oldest rocks in the eastern SRP basin have not been penetrated by drilling. Instead, two deep drill holes located south of the Lemhi Range on the eastern SRP provide partial evidence of the subsidence history of the eastern SRP. As shown in Figure 15, holes WO-2 and INEL-1 penetrated the basalt sequence and terminated in altered rhyolite. New ages of 8.0 and 8.5 Ma (SHRIMP U-Pb, zr) were obtained from rhyolite at depths of 1,482 m and 3,060 m in hole INEL-1 (M. McCurry, oral commun., 1999). These ages differ from preliminary fission track ages of identical rocks (Morgan and others, 1984) but are believed to be more accurate based on the improved methodology.

A rock subsidence curve can be compiled using the age-depth relations of volcanic rocks in INEL-1 and WO-2 (Figure 16). According to these data, 3.1 km of subsidence occurred since 8.5 Ma, and the remaining subsidence (between 1.4 and 4.4 km) occurred before 8.5 Ma. The smooth curve shown in Figure 16 indicates rapid (1.5 km/m.y.) subsidence before 8 Ma and slow (0.2 km/m.y.) subsidence since 8 Ma. If subsidence at INEL-1 was due to regional processes, the curve implies that regional eastern SRP subsidence started about 10 Ma. Alternatively, the rapid accumulation rate, rock texture (Morgan and others, 1984), and absence of correlative rocks in nearby ranges may be evidence that INEL-1 rhyolitic rocks accumulated in a fault-bounded basin, perhaps a caldera. In this scenario, the INEL-1 ages record significant local subsidence between 8.5 and 8 Ma and about 1.7 km of regional subsidence since 8 Ma. In this interpretation, most of the calculated regional subsidence (between 2.8 and 5.8 km) occurred before 8 Ma but is not manifested in the drill hole data.

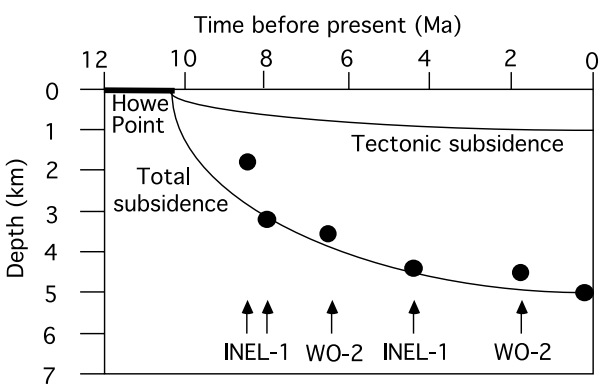

Figure 16. Eastern SRP subsidence graph constrained by INEL-1 and WO-2 well log data. Figure assumes 5 km of subsidence measured relative to correlative rocks in the adjacent Basin and Range (see Figure 13). The total subsidence is a combination of tectonic subsidence (due to midcrustal densification) and subsidence due to the weight of basin-filling volcanic and sedimentary rocks. Age-depth relations in WO-2 are from Hackett and others (1994) and Anderson and others (1997). Other data are from McBroome (1981), Morgan and others (1984), and M. McCurry (oral commun., 1999). Initial subsidence at Howe Point (16-10 Ma) from Figure 7.

SURFACE SUBSIDENCE AND TECTONIC GEOMORPHOLOGY

The eastern SRP and surrounding regions are characterized by axial drainage, wherein tributary streams flow toward the eastern SRP and its trunk river, the Snake River, which itself flows southwest along the axis of the eastern SRP. This geomorphic system reflects tectonic processes, including first-order surface subsidence and second-order fault and volcanic rift patterns, and climatic processes. Because the drainage system is strongly influenced by regional surface subsidence, we can use it to study subsidence through time. In particular, the extent and initiation of surface subsidence should be recorded by the extent and age of axial drainage development. To this end, a region immediately south of the eastern SRP was studied to describe landscape evolution during eastern SRP development. The study area encompasses Arbon Valley to the Portneuf Range including two streams, the Portneuf River and Bannock Creek (Figure 2).

Maximum Basin Filling

A low gradient surface is perched at higher elevations in the northern Bannock Range (Figure 17), as much as 900 m above the eastern SRP. Near Kinport Peak, the surface cuts across tilted Proterozoic rocks, whereas to the south it cuts across tilted Miocene basin fill. The surface is generally undissected by modern streams and is overlain by rare but distinctive white quartzite cobbles derived from the Ordovician Swan Peak Quartzite. The surface is fringed by dissected, lower-elevation terrain

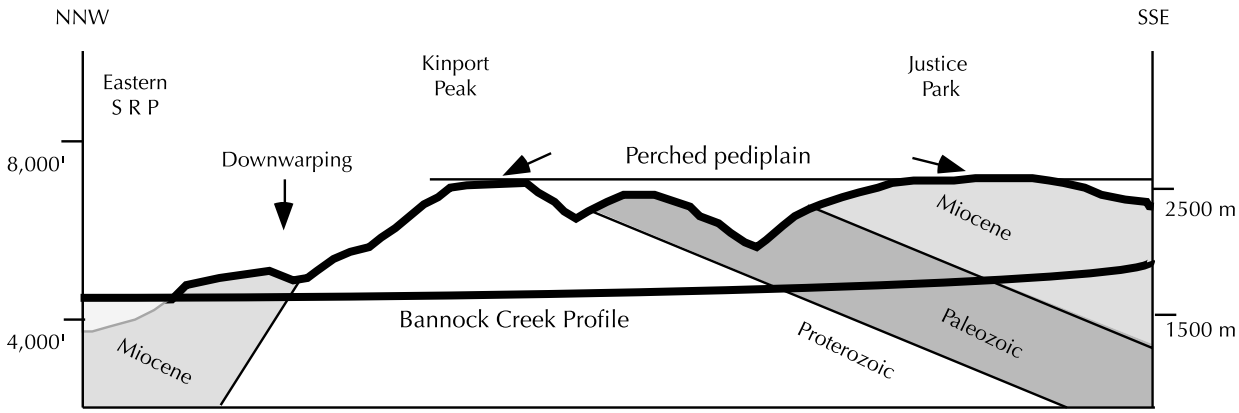

Figure 17. Schematic cross-section of high-level pediplain surface in northern Bannock Range. Surface is at an elevation of about 7,200 feet and cuts across east-tilted Proterozoic, Paleozoic, and Miocene rocks. South of Kinport Peak, the vertical distance between the mountain profile and the superimposed Bannock Creek profile represents the maximum incision interpreted for valleys like Arbon Valley and Portneuf Valley. North of Kinport Peak, crustal flexure and downwarping has occurred. Location of cross section shown in Figure 2. Vertical exaggeration is about 5.

that ultimately grades to the Portneuf River and Bannock Creek.

The perched surface and overlying cobbles are interpreted to be a regional pediplain with lag concentrate resulting from fluvial processes. The surface, although discontinuous and irregular today, must have been laterally continuous across the northern Bannock Range and must have formed after Basin and Range tilting was completed (post-7.3 Ma; Figure 9). The profound implication is that after Basin and Range faulting ceased the top of the northern Bannock Range and the Portneuf and Arbon valleys were at the same elevation as one another and as the eastern SRP. Miocene basin fill must have filled the valleys to the tops of the intervening ranges, 800 to 900 m above the modern valley floors. An alternative explanation, that the terrace was uplifted relative to the modern valleys during renewed Basin and Range faulting, is untenable because (1) basin fill is present immediately below the terrace, (2) the terrace is at similar elevations on either side of a major Basin and Range fault, and (3) the horizontal terrace shows no indication of eastward tilting that would accompany faulting. Our preferred interpretation is that basin fill accumulated to the level of the pediplain and that this low-relief surface may have been graded to the eastern SRP before its surface subsided, or to a regional base level to the east. Paleocurrent information relating to processes on this surface has not been found.

Basin Emptying

The Bannock and Portneuf rivers are consequent streams that flow north to the Snake River. The rivers flow parallel to the structural grain imparted by rocks

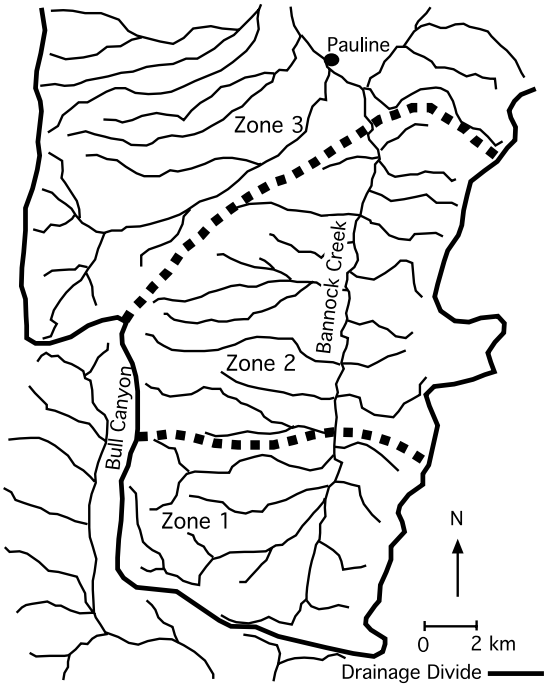

Figure 18. Bannock Creek drainage patterns in southern Arbon Valley. Location shown in Figure 2. Tributary streams in zone 1 have "barbed" confluence angles with Bannock Creek, and other streams undergo an abrupt change in direction from south to north. Tributaries show perpendicular confluence angles in zone 2 and acute confluence angles in zone 3. A related geomorphic feature is the offset drainage divide in the Deep Creek Range: Knox Canyon discharges into Arbon Valley, and Bull Canyon discharges south into the Bonneville Basin, but the divide that separates the two is 10-12 km north of the Arbon Valley divide. The drainage patterns are interpreted to reflect headward (southward) erosion of Bannock Creek. Headward migration and progressive stream capture are recorded where streams incise nonresistant gravels, but where streams incise resistant bedrock the divide is relatively fixed. The Arbon Valley divide has migrated 10 km south since incision into bedrock and about 23 km south since the early to middle Pleistocene terraces of Arbon Valley were formed. From Bobo (1991).

and faults, preferentially incising nonresistant late Cenozoic basin fill and impeded by bedrock horsts. By incising the land, they have created subsequent valleys such as the Marsh Creek, Portneuf, and Arbon valleys (Figure 2). In these young valleys, Miocene basin fill from 0 to 600 m below the pediplain is generally absent, and basin fill from 600 to 900 m below the surface is partially incised or concealed beneath younger deposits.

We attribute valley incision to surface subsidence of the eastern Snake River Plain and the ancestral Snake River that flowed over it; the reduction in base level of the Bannock and Portneuf rivers induced significant downcutting by these tributary streams. In this scenario, widespread erosion occurred first but was later replaced by several smaller cut-and-fill cycles, which we interpret to reflect the second-order effects of Pleistocene climate change and basaltic volcanism on the eastern SRP.

The age of incision and inferred surface subsidence has not been systematically studied. Incision by the Portneuf River system began after 7.3 Ma, the youngest age of basin fill beneath the pediplain. About 700 m of incision was completed before a prominent bajada surface developed along the Portneuf River, which is interpreted to be early to middle Pleistocene (Scott, 1982). About 900 m of incision was completed when the ancestral Portneuf River channel was filled by the Portneuf Valley basalt, which yielded a whole rock K-Ar date of 580 Ka (Pierce and Scott, 1982). The base of the basalt is at the same level as the modern Portenuf River, evidence of minimal incision since that time. The age of incision by Bannock Creek is partially recorded near its headwaters, where the drainage pattern is interpreted to record 23 km of headward migration induced by base level change (Figure 18; Bobo, 1991). Because the incised substrate is alluvial gravel of early to middle Pleistocene age (Scott, 1982), migration is interpreted to be the result of middle to late Pleistocene surface subsidence of the eastern SRP. Other mechanisms of base level change, such as localized incision of eastern SRP basalts by the Snake River or pluvial lake formation in the Bonneville Basin, may have been contributing factors as well.

DISCUSSION

CRUSTAL DEFORMATION MODEL

In an earlier paper (Rodgers and others, 1990, p. 1,140), we proposed a model of eastern SRP deformation that emphasized extension and the role of a mantle plume:

East of the locus of volcanism, the crust extended by normal faulting at shallow levels and ductile attenuation at depth. Sedimentary basins formed and were filled by horst-derived clastic detritus. Basins east-northeast of the locus of volcanism were progressively obliterated as the continent drifted over the plume, but basins north or south of the path of volcanism were preserved. Over the plume, the crust extended by normal faulting at very shallow levels and magma injection at depth. North and south of the plume, the crust continued to extend by faulting and ductile attenuation, resulting in basins filled with plume-derived volcanic detritus. West of the plume, minor extension in the volcanic province was accommodated by the injection of basalt dikes and by rare normal faults.

Some revision of this model is needed to account for the space-time patterns of extension and subsidence summarized in this paper and by Pierce and Morgan (1992) and McQuarrie and Rodgers (1998). As before, deformation is described in relation to transgressing silicic volcanism (Figure 19). Data and interpretations used to build the new model are summarized in Figure 20, and the new model is illustrated in Figure 21 and described below. The model is predicated on the interpretation that rocks and structures similar to those beside the eastern SRP were formerly present on the eastern SRP, but have since subsided and been covered by younger volcanic and sedimentary rocks.

Stage 1 (16-11 Ma)

In the initial stage of deformation, the “proto-eastern SRP” was characterized by half-graben development. Basin fill included thin sequences of carbonate rocks, fine-grained clastic rocks, air-fall tuff and rare basalt that compose the Beaverdam Formation in Goose Creek, the lower Starlight Formation in Arbon Valley, the Medicine Lodge beds throughout the northeast margin of the eastern SRP, and the Teewinot Formation in Jackson Hole. The rocks accumulated in lacustrine and fluviolacustrine environments and were flanked by mountains or highlands, as shown by the uncommon intercalation of pebble conglomerate and by regional facies patterns in at least two basins (Goose Creek and Birch Creek) indicative of Basin and Range morphology. Sedimentation rates of 50-80 m/m.y. are interpreted to reflect slow basin subsidence due to slow rates of extension. Available age constraints (Figure 9) indicate the basins existed from 16 to 9 Ma overall, with basin initiation from 16 to about 11 Ma and an east-migrating basin cessation from 11 to 9 Ma.

Rocks in the lower Starlight Formation and Medicine Lodge beds are not areally restricted to individual half grabens, but they are restricted to the margins of the east-

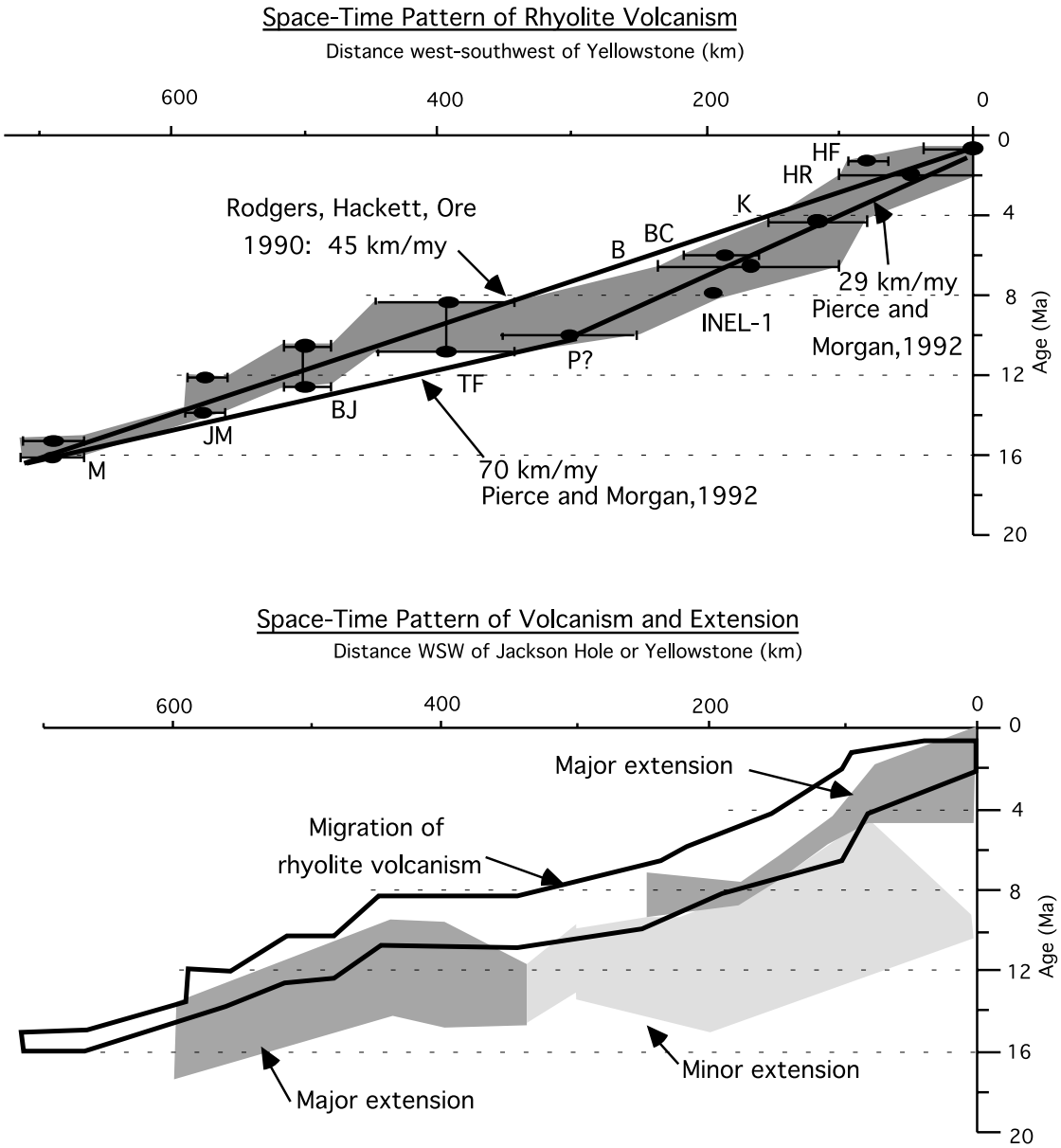

Figure 19. Space-time pattern of rhyolite magmatism and its relation to extension (see Figure 9). The duration of rhyolite magmatism from the Owyhee Plateau to Yellowstone Plateau is shown, including the following volcanic fields and calderas: McDermitt (M), Juniper Mountain (JM), Bruneau-Jarbidge (BJ), Twin Falls (TF), Picabo (P), INEL-1 drill hole, Blacktail (B), Blue Creek (BC), Kilgore (K), Huckleberry Ridge (HR), Henry's Fork (HF), and Yellowstone. The eastward migration of silicic magmatism is a first-order pattern of the eastern SRP, supported by most data with the following caveats: (1) well WO-2 on the INEEL was drilled within the inferred caldera of the 6.6 Ma tuff of Blacktail but met a Blacktail outflow sheet instead of intracaldera fill (Hackett and others, 1994); (2) wells INEL-1 and WO-2 intersected thick rhyolite units that were previously undocumented along the eastern SRP margins (Hackett and others, 1994, M. McCurry, oral commun., 1999) indicating the marginal record is incomplete here and possibly elsewhere; (3) the 10.2 Ma tuff of Arbon Valley (from the Picabo caldera) is petrologically distinct (Trimble and Carr, 1976; Kellogg and others, 1994) and perhaps petrogenetically distinct from other eastern SRP rhyolites; and (4) silicic magmatism was widespread across the central and eastern SRP from 8.5-11.5 Ma. Neogene rhyolite magmatism migrated northeast at a constant rate (Armstrong and others, 1975; Rodgers and others, 1990) or two constant rates before and after 10 Ma (Pierce and Morgan, 1992). Note that the difference between Pierce and Morgan's volcanic migration rate (29 ± 5 km/m.y.) and the Basin and Range extension rate (4-6 km/m.y; see Figure 4) is equivalent to the independently calculated North America plate migration rate of 22 ± 8 km/m.y. (Gripp and Gordan, 1990), evidence in support of a hot-spot origin for the eastern SRP. Sources of data include Bonnichsen (1982), Christiansen (1984), Ekren and others (1982, 1984), Kellogg and others (1994), Morgan and others (1984), Perkins and others (1995), Pierce and Morgan (1992), Rytuba and McKee (1984), and sources listed in Figure 9.

ern SRP. In addition, the age and lithologies of these two units are identical at two points (Trail Creek and Howe Point; Figure 2) on opposite margins. A speculative hypothesis is that the smaller half-graben basins were integrated across the proto-eastern SRP, and that integration was due to regional subsidence. Documenting regional subsidence during stage 1 would be significant because it could relate stages 1 and 2: Subsidence was induced by regional dike injection and densification of the crust, which heated and weakened the lower crust allowing the upper crust to fail in extension and form minor half grabens. After a few million years of dike injection, regional

Feature	Description	Evidence	Reference
Late Quaternary Rift Zones			
Width and distribution	Narrow, discrete	Exposed vents and fisures	1
	Broad, diffuse	Exposed and subsurface vents	2
Extension direction	W to WSW	Trend of rift zones	
Extension amount	Unknown		
Neogene-Late Quaternary Normal Faults			
Cumulative extension			
Direction	W to WSW	Strike of normal faults	
Amount	20% (south), 10-15% (north)	Restored cross sections	Figs. 3 & 4; 4
Older extension			
Amount	Inferred minor	Thin, fine-grained clastic and carbonate basin fill Sedimentation rates of 50-80 m/m.y.	3
Age	Migrated ENE through time began 16 to 10 Ma ended 11 to 9 Ma	Age of basin fill, south margin	Fig. 9
Relation to volcanism	Prior to initial silicic eruptions	Space-time pattern	Fig. 19
Younger extension			
Amount	Inferred major	Thick, coarse-grained clastic basin fill Sedimentation rates of 100-300 m/m.y.	3
Age	Migrated ENE through time began 10 Ma, ongoing today	Age of basin fill, south margin	Fig. 9 5, 6
	Migrated outward from SRP	Age pattern of rapid tilting of basin fill	7
Relation to volcanism	Preceding and beside initial silicic eruptions	Space-time pattern	Fig. 19
Neogene-Quaternary Rock Subsidence			
Amount	4.5 to 8.5 km Decreases north to south(?) Increases near Pleistocene rifts	Crustal flexure, north margin	8
Age	Began 16-10 Ma, ongoing today	Howe Point unconformity	Fig. 7
Rate	Decreases through time	Subsidence curve	Fig. 16
Relation to magmatism	Coeval and after silicic eruptions	Age-depth relations in INEL-1 drill hole	Fig. 15
	Coeval with midcrustal intrusion Coeval with basaltic eruptions	Subsidence model	8
Neogene-Quaternary Surface Subsidence			
Amount	900 m Unknown along north margin	Pocatello perched pediplain, incised valleys	Fig. 17
Age	Younger than 7.3 Ma	Age of basin fill below Pocatello terrace	3
Relation to volcanism	After silicic eruptions Coeval with basaltic eruptions	Age of rhyolite near Pocatello	

References:
(1) Kuntz, 1992; (2) Wetmore and others, 2000; (3) this paper; (4) Janecke, 1993; (5) Rodgers and others, 1990; (6) Pierce and Morgan, 1992; (7) Anders and others, 1989; (8) McQuarrie and Rodgers, 1998

Figure 20. Summary of Miocene to Quaternary deformation, eastern SRP.

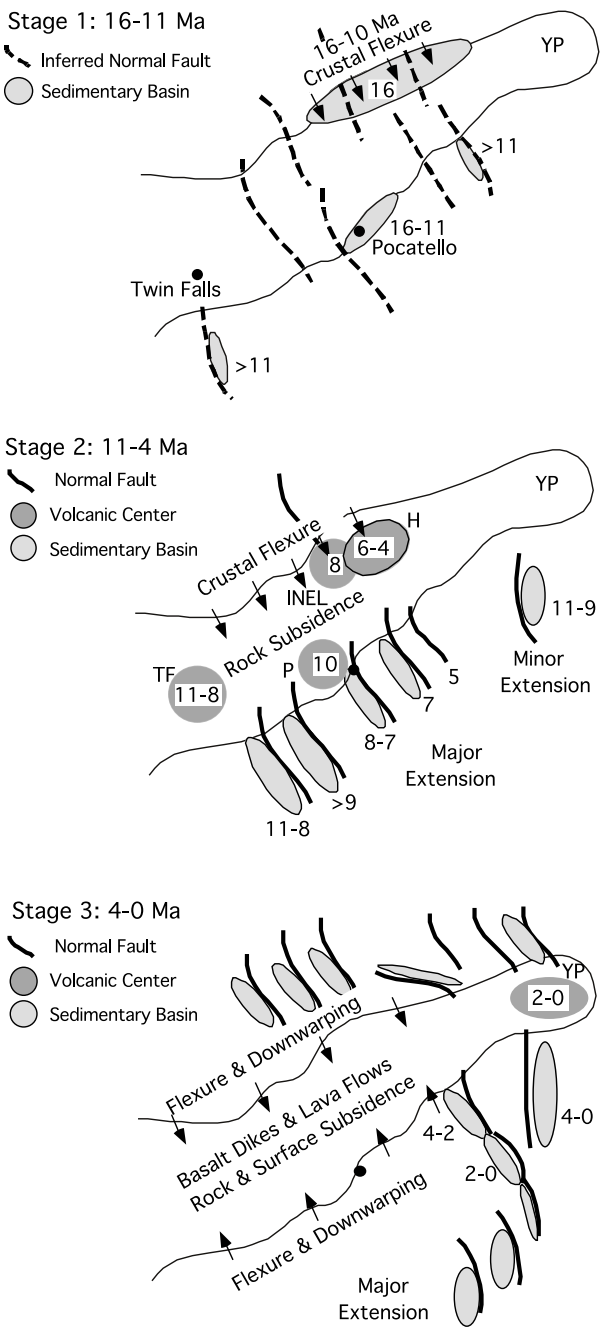

Figure 21. Schematic maps of the eastern SRP showing the space-time pattern of extension, subsidence, sedimentation, and volcanism during deformational stages 1, 2, and 3. The ages (shown in millions of years) associated with each deformational event are useful approximations, but because of the transgressive nature of tectonism they may not be accurate for all locations. Major silicic volcanic centers include Twin Falls (TF), Picabo (P), INEL-1 drill hole (INEL), Heise (H), and Yellowstone Plateau (YP). Data and references presented in Figures 9 and 19.

subsidence, and upper crustal extension, partial melting of the lower crust created silicic melts that erupted periodically across the region during stage 2.

Stage 2 (11-4 Ma)

In the second stage of deformation, a major pulse of extension swept eastward from longitude 115° to its current position on the Yellowstone Plateau. The upper crust extended by normal faulting, and the lower crust presumably extended and thinned by lower crustal flow and dike injection. Extension is manifested along the eastern SRP margins by half grabens with distinctively thick sequences of clastic rocks including the upper Starlight Formation in Raft River Valley, Rockland Valley, Arbon Valley, Portneuf Valley, and Buckskin Basin. Sedimentation rates of 100-300 m/m.y. are interpreted to reflect rapid subsidence and rapid rates of extension. Extension is also manifested by normal faults in the Blackfoot Mountains, by rapidly tilted basin fill in Swan Valley, Grand Valley, and Jackson Hole, and by current patterns of seismicity, elevation, and Quaternary faults in the circum-eastern SRP. Cumulative extension along the eastern SRP margins, which decreases slightly from south (20 percent) to north (10-15 percent), mostly occurred during this event. The extension rate was 4-6 km/m.y. from 11 to 0 Ma (depending upon how much extension occurred from 16-11 Ma versus 11-0 Ma). As measured along the southern margin of the eastern SRP, this extensional event migrated eastward from 11 to 0 Ma, preceding and beside initial silicic magmatism at any one place on the eastern SRP (Rodgers and others, 1990; Pierce and Morgan, 1992). Based only on data from southern Birch Creek Valley (Figure 7; Rodgers and Anders, 1990), extension was coeval along the north margin.

The eastern SRP experienced significant rock subsidence with respect to the adjacent Basin and Range. At least 4.5 km total subsidence occurred near the north margin and was accommodated by a narrow zone of crustal flexure and northeast-striking normal faults. Rock subsidence along the southern margin has not been studied, although northeast-striking normal faults and downwarping are widespread there. Regional subsidence was driven by the emplacement of dense mafic dikes and sills in the middle crust and accentuated by the accumulation of volcanic and sedimentary rocks on the surface (Figure 16). Most of the subsidence along the north margin occurred during or before local silicic magmatism from 8.5 to 6.0 Ma (Figure 21), evidence that the midcrustal sill formed during or before the pulse of silicic magmatism.

Silicic volcanism and thermal expansion may have

created a (migrating?) topographic highland, similar to the modern Yellowstone Plateau, across some of the eastern SRP (Fritz and Sears, 1993), but more paleocurrent data from marginal half-graben basin fill are needed to document this. East of and beside silicic volcanism on the plain, half grabens that formed during the extensional pulse probably created a rugged Basin and Range topography characterized by north-trending valleys and mountains. However, the rugged landscape experienced truncation and filling near the end of Stage 2 as shown by the presence of a regional pediplain across mature half grabens in the northern Bannock Range.

Stage 3 (4-0 Ma)

In the third stage of deformation, the eastern SRP has experienced dike injection, rock subsidence, and surface subsidence. Extension via upper crustal dike injection has occurred beneath volcanic rift zones (Rodgers and others, 1990; Hackett and others, 1996). Exposed rift zones are rather sharply defined (Kuntz and others, 1992), but the distribution of late Pleistocene subsurface vents is more diffuse (Hughes and others, this volume). The direction of extension changes within the southeastern half of the eastern SRP: ranges south of here trend north, whereas volcanic rift zones north of here trend northwest, and the Great Rift itself bends in this region (Pierce and Morgan, 1992, and references therein). The amount of extension shows a similar pattern of change. The southeastern edge of the eastern SRP appears to be the locus of lowest strain, with extension increasing gradually and symmetrically away to the arcuate zones of seismicity, high topography, and active Quaternary faults documented by Anders and others (1989) and Pierce and Morgan (1992). Indeed, calculations suggest that the amount of strain via dike injection on the plain is the same order of magnitude as that accommodated by normal faults north of the plain (Parsons and others, 1998).

Rock subsidence has continued during stage 3, but the amount and rate of subsidence (about 1,000 m in 4 m.y.) have been significantly less than that during stage 2. Quaternary subsidence is indicated along the northern margin of the plain where flexure contours define a pattern of reentrants that coincide with late Quaternary volcanic rift zones (Figure 12), and along the south margin where the Pleistocene Raft Formation is gently tilted northward (Houser, 1992). Cumulative rock subsidence has been at least 4.5 km, evidence of a midcrustal dike and sill complex at least 17 km thick. As in stage 2, subsidence during stage 3 has been accommodated at deeper levels by the ductile flow of lower crust to the Basin and Range from the eastern SRP.

Surface subsidence and the emplacement of basalt lava flows have created the modern eastern SRP during stage 3. Surface subsidence is manifested by downwarping of rocks along both margins of the plain, by axial drainage throughout the region, by as much as 900 m of incision of a perched pediplain near Pocatello, by drainage reversals of streams tributary to the Snake River, and by theodolite surveys of the modern surface (Reilinger and others, 1977). The age of surface subsidence is only known to be younger than 7.3 Ma, although further study may significantly improve the constraints. Basalt thins and the plain increases in elevation to the east (Brott and others, 1981), evidence of an eastward migration of basalt volcanism and subsidence during stage 3.

CRITIQUE OF TECTONIC MODELS

The revised deformation model can be used to test various tectonic models for the origin of the province. Tectonic models for the origin and development of the SRP-Yellowstone system include a propagating rift (Hamilton, 1987; 1989), a crustal flaw (Eaton and others, 1978), a transform fault (Christiansen and McKee, 1978), an origin by meteorite impact (Alt and others, 1988), a hot-spot track (Morgan, 1972; Suppe and others, 1975; Pierce and Morgan, 1992, and references therein), and a self-propagating convective melt (Saltzer and Humphreys, 1997). All but the last model were critiqued in detail by Pierce and Morgan (1992), who concluded that a two-phase hot-spot model was uniquely supported by most of the magmatic, deformational, geophysical, and sedimentary data. Without repeating the discussion of Pierce and Morgan (1992), what follows is a brief critique of the tectonic models (except the crustal flaw and meteorite impact models, for which we have no relevant data) based upon the space-time relations described in this paper.

Eastward-Propagating Rift

We have found no faults that accommodated downfaulting of the eastern SRP, nor have we observed northeast-striking dikes while mapping along its margins. Flexure along its margins is similar to monoclines that border a few rifts (Sengor, 1995), but flexure is interpreted to reflect vertical subsidence of the eastern SRP without horizontal (NW-SE) extension. In a few localities, we have documented mutual cross-cutting relations between Basin and Range faults and flexure-related normal faults, indicating NE-SW extension and crustal flexure occurred synchronously. Eastern SRP-parallel normal faults in the adjacent Basin and Range Province show only minor offset and are interpreted to be a consequence

of crustal flexure (Zentner, 1988), not regional NW-SE extension. Overall, the structural data of the region provide little support for interpreting the eastern SRP as an eastward-propagating extensional rift (Hamilton, 1987, 1989).

Transform Fault at the Northern End of the Basin and Range

Nowhere along the margins of the eastern SRP have we or others identified eastern SRP-parallel strike-slip faults, orographic bending, or minor pull-apart basins that would indicate lateral offset of the crust (see discussion in Pierce and Morgan, 1992). The amount of Basin and Range extension diminishes slightly to the north, and the direction changes by 30 degrees, but these are small differences that do not require a transform system. Crustal flexure has affected both margins of the eastern SRP: documented flexure on the north side appears greater than the estimated flexure on the south side, but again the small difference in kinematics does not require a transform system. Further work is needed to document the inception of Basin and Range faulting on the north side of the eastern SRP and to seek a significant age difference between initial extension on the north and south, but the available data are in favor of a broadly symmetrical pattern of extension and subsidence through time.

Mantle Plume or Self-Propagating Convective Instability

Much of the history outlined in this paper is compatible with previously proposed models that the eastern SRP marks the passage of North America over a mantle plume (Pierce and Morgan, 1992, and references therein) or self-propagating convective instability (Saltzer and Humphreys, 1997), now located beneath the Yellowstone Plateau. In particular, these models are well-supported by the space-time patterns of extension, subsidence, and tectonic geomorphology manifested during stages 2 and 3 of the deformation model presented above. The models differ from one another in mantle dynamics and kinematics: the plume model incorporates a deep mantle source, whereas the instability model involves lengthwise convection cells in the asthenospheric mantle that are instigated by lithospheric shear (Saltzer and Humphreys, 1997). However, the models as currently conceived are indistinguishable in crustal dynamics and kinematics: the crust of the eastern SRP, Yellowstone Plateau, and adjacent Basin and Range would host the same deformational processes and experience the same deformational history in either case.

We conclude by emphasizing that whatever tectonic model is ultimately chosen for the eastern SRP, that model must incorporate crustal deformation before silicic volcanism. Half-graben normal faulting occurred in front of and prior to silicic volcanism in any one location. Regional rock and surface subsidence may have preceded silicic volcanism as well, although more evidence is needed to document this process. The leading edge of the migrating Yellowstone system was manifested on the surface by crustal extension and basin formation, and possibly by mafic plutonism at depth.

SUGGESTIONS FOR FUTURE WORK

The deformational model outlined in this paper is supported by evidence of the style, kinematics, and timing of extension and subsidence observed in isolated places along the margins of the eastern SRP. The model should be tested and revised by completing similar studies in many more places along the margins. Some suggestions include:

(1) Determine the ages of initial and rapid extension along the north margin of the eastern SRP by describing and dating half-graben basin fill in several locations and by measuring the angular unconformities between different units.

(2) Estimate the amount of crustal flexure along the south margin by measuring fold plunges or tilted Miocene rocks and calculating a best-fit flexural curve.

(3) Estimate the rate of crustal flexure along the north and south margins by measuring the angularity across unconformities in differentially flexed Neogene rocks.

(4) Document the age and amount of surface subsidence along the south and north margins wherever appropriate erosional surfaces are preserved.

(5) Study the stratigraphy and sedimentology of the Medicine Lodge beds and lower Starlight Formation to characterize the tectonic setting of the eastern SRP before silicic volcanism initiated.

(6) Complete high resolution gravity studies of the eastern SRP to identify concealed half grabens beneath the volcanic rocks.

(7) Obtain precise ages on basalt and rhyolite in drill holes on the eastern SRP to better define age-depth relations and to document the initial age of voluminous basalt eruptions.

COMMENTS ON RESEARCH SINCE MANUSCRIPT ORIGINALLY SUBMITTED

Additional data and interpretations about deforma-

tion near the eastern SRP have been presented since our paper was written and submitted over five years ago. Janecke and others (2000) discuss eastern SRP-parallel normal faults of the northeastern Basin and Range Province. Whereas Zentner (1988) documented late Cenozoic activity on faults within 30 km of the eastern SRP, Janecke and others (2000) identified late Cenozoic movement on faults farther from the plain. They proposed that crustal subsidence within the arc of high topography and seismicity has induced a secondary strain field, characterized by approximately plain-perpendicular extension, that is superimposed on the Basin and Range strain field. This model is compatible with the one proposed by Zentner (1988) and discussed in our paper, if two strain fields exist in association with two wavelengths of crustal flexure. Both strain fields involve plain-perpendicular extension, but the amount of extension is much smaller than the amount of plain-parallel "Basin and Range" extension.

Hough (2001) addresses the age and rate of crustal flexure in the Lidy Hot Springs region (Figure 2) along the northeastern margin of the eastern SRP. He measured the plunges of six map-scale fold hinges in Paleozoic rocks and used these to locate a flexural hinge that roughly parallels the eastern SRP margin. The flexural hinge separates horizontal folds (to the north) from folds with 25-degree southward plunges (to the south), similar to the one identified by McQuarrie and Rodgers (1998). Hough (2001) found that the Medicine Lodge beds, which overlie the folded Paleozoic rocks, have the same orientation north and south of the flexural hinge, evidence that the Medicine Lodge beds postdate the flexure recorded by Paleozoic folds. The Medicine Lodge beds in this region are undated, but inferred to be middle Miocene (Skipp and others, 1979), and contain tuff that is chemically similar to eastern SRP tuffs (Hough, 2001). Hough also recognized disconformable contacts between Medicine Lodge beds and overlying 6.6-6.2 Ma volcanic rocks, and a minor amount of post-6.2 Ma eastward tilting. Hough proposed a Neogene history that includes the deposition of the Medicine Lodge beds at Howe Point (about 16 Ma), an initial pulse of southward flexure everywhere along the eastern SRP margin (between 16 and 10 Ma according to Figure 7), the deposition of the Medicine Lodge beds at Lidy Hot Springs, the emplacement of 6.6 to 6.2 Ma volcanic rocks everywhere along the eastern SRP margin, and the eastward tilting of Lidy Hot Springs rocks due to Basin and Range faulting. This history matches that of deformation proposed in our paper and awaits confirmation by dates on the Medicine Lodge beds at Lidy Hot Springs.

Kuntz and others (2002) analyze exposed structures of the eastern SRP, including tension cracks, eruptive fissures, concealed dikes, and faults. Their mapping shows that dike systems of the eastern SRP average 20 km long but may be as much as 40 km long. They interpreted some structures, like the Arco rift zone, to represent continuations of normal faults adjacent to the eastern SRP.

The Big Lost trough has recently been defined by Geslin and others (2002) and Bestland and others (2002) as a subbasin of the eastern SRP. With upper Pliocene-Quaternary rocks as much as 200 m deeper than correlative rocks beyond the subbasin, the Big Lost trough provides evidence of non-uniform subsidence across the eastern SRP. The trough is located immediately south of the Lost River Range, coincident with the greatest amount of crustal flexure along the eastern SRP margin (Figure 13).

Humphreys and others (2000) propose that Yellowstone tectonism is intricately related to the progression of magmatism across the High Lava Plains of Oregon, because the bilateral symmetry of this broader tectonic system argues against a simple hotspot origin for the Yellowstone system. Expanding upon the model of Saltzer and Humphreys (1997), they proposed that partial melting beneath these two magmatic tracks has left a residuum of uppermost mantle. This residuum would block the rise of underlying hot, fertile mantle rock, causing it to be bilaterally deflected to the leading tips of the two tracks. The larger volume of magma along the Yellowstone track is attributed in part to greater crustal extension there than in eastern Oregon. With regard to the Yellowstone-eastern SRP, this model differs from the hotspot model in mantle dynamics but not in crustal dynamics, and it is compatible with the deformational processes described in this paper.

ACKNOWLEDGMENTS

This research was supported by grants from the Idaho State Board of Education and NASA Idaho Space Grant Consortium. The authors thank Geology faculty and students at Idaho State University for provocative discussions and the 1993 Advanced Structure class for compiling regional cross sections through southeastern Idaho. Thanks also to Bill Hackett, Roger Stewart, and Bill Bonnichson for detailed reviews that added clarity and focus to the paper.

REFERENCES

Albee, H.F., and H.L. Cullins, 1965, Preliminary map of the Poker Peak and Palisades Reservoir quadrangles, Bonneville County, Idaho, and Lincoln County, Wyoming: U.S. Geological Survey Geologic Map GQ-1260.

Allmendinger, R.W., 1982, Sequence of late Cenozoic deformation in the Blackfoot Mountains, southeastern Idaho, *in* Bill Bonnichsen and R.M. Breckenridge, eds., Cenozoic Geology of Idaho: Idaho Bureau of Mines and Geology Bulletin 26, p. 505-516.

Alt, David, J.M. Sears, and D.W. Hyndman, 1988, Terrestrial maria: The origins of large basalt plateaus, hotspot tracks and spreading ridges: Journal of Geophysical Research, v. 96, p. 647-662.

Anders, M.H., 1990, Late Cenozoic evolution of Grand and Swan Valleys, Idaho, *in* Sheila Roberts, ed., Geologic Field Tours of Western Wyoming and Parts of Adjacent Idaho, Montana, and Utah: Geological Survey of Wyoming Public Information Circular 29, p. 15-25.

———, 1994, Constraints on North American plate velocity from the Yellowstone hotspot deformational field: Nature, v. 369, p. 53-55.

Anders, M.H., J.W. Geissman, L.A. Piety, and J.T. Sullivan, 1989, Parabolic distribution of circum-eastern Snake River Plain seismicity and latest Quaternary faulting: Migratory pattern and association with the Yellowstone hotspot: Journal of Geophysical Research, v. 94, p. 1589-1621.

Anders, M.H., and N.H. Sleep, 1992, Magmatism and extension: The thermal and mechanical effects of the Yellowstone hotspot: Journal of Geophysical Research, v. 97, p. 15,379-15,394.

Anders, M.H., Mark Spiegelman, D.W. Rodgers, and J.T. Hagstrum, 1993, The growth of fault-bounded tilt blocks: Tectonics, v. 12, p. 1451-1459.

Anderson, S.R., and M.J. Liszewski, 1997, Stratigraphy of the unsaturated zone and the Snake River Plain aquifer at and near the Idaho National Engineering Laboratory, Idaho: U.S. Geological Survey Water-Resources Investigations Report 97-4183, 65 p.

Armstrong, F.C., 1969, Geologic map of the Soda Springs quadrangle, southeastern Idaho: U.S. Geological Survey Miscellaneous Investigations Map I-557, scale 1:48,000.

Armstrong, R.L., W.P. Leeman, and H.E. Malde, 1975, K-Ar dating, Quaternary and Neogene volcanic rocks of the Snake River Plain, Idaho: American Journal of Science, v. 275, p. 225-251.

Armstrong, R.L., J.F. Smith, H.R. Covington, and P.L. Williams, 1978, Preliminary geologic map of the west half of the Pocatello 1º x 2º quadrangle, Idaho: U.S. Geological Survey Open-File Report 78-1018, scale 1:250,000.

Barrientos, S.E., R.S. Stein, and S.N. Ward, 1987, Comparison of the 1959 Hebgen Lake, Montana, and the 1983 Borah Peak, Idaho, earthquakes from geodetic observations: Bulletin of the Seismological Society of America, v. 77, p. 784-808.

Bestland, E.A., P.K. Link, M.A. Lanphere, and D.E. Champion, 2002, Paleoenvironments of sedimentary interbeds in the Pliocene and Quaternary Big Lost trough, eastern Snake River Plain, Idaho, *in* P.K. Link and L.L. Mink, eds., Geology, Hydrogeology, and Environmental Remediation: Idaho National Engineering and Environmental Laboratory, Eastern Snake River Plain, Idaho: Geological Society of America Special Paper 353, p. 27-44.

Blackwell, D.D., Shari Kelley, and J.L. Steele, 1992, Heat flow modeling of the Snake River Plain, Idaho: U.S. Department of Energy Report for contract DE-AC07-761DO1570, 109 p.

Bobo, R.T., 1991, Basin evolution of Arbon Valley and its relation to Snake River Plain volcanism and Basin and Range tectonics: Idaho State University M.S. thesis, 82 p.

Bonnichsen, Bill, 1982, The Bruneau-Jarbidge eruptive center, southwestern Idaho, *in* Bill Bonnichsen and R.M. Breckenridge, eds., Cenozoic Geology of Idaho: Idaho Bureau of Mines and Geology Bulletin 26, p. 237-254.

Braile, L.W., R.B. Smith, J. Ansorge, M.R. Baker, M.A. Sparlin, C. Prodehl, M.M. Schilly, J.H. Healy, S. Mueller, and K.H. Olsen, 1982, The Yellowstone-Snake River Plain seismic profiling experiment: Crustal structure of the eastern Snake River Plain: Journal of Geophysical Research, v. 87, no. B4, p. 2597-2609.

Brott, C.A., D.D. Blackwell, and J.P. Ziagos, 1981, Thermal and tectonic implications of heat flow in the eastern SRP, Idaho: Journal of Geophysical Research, v. 86, no. B12, p. 11,709-11,734.

Bruhn, R.L., D. Wu, and J-J. Lee, 1992, Final report on structure of the southern Lemhi and Arco fault zone, Idaho: Informal report contract no. EGG-NPR-10680, 25 p.

Burgel, W.D., 1986, Structural geology of the Rapid Creek area, Pocatello Range, north of Inkom, southeast Idaho: Idaho State University M.S. thesis, 72 p.

Burgel, W.D., D.W. Rodgers, and P.K. Link, 1987, Mesozoic and Cenozoic structures of the Pocatello region, southeastern Idaho, *in* W.R. Miller, ed., The Thrust Belt Revisited: Wyoming Geological Association, 37th Annual Field Conference Guidebook, p. 91-100.

Carlson, R.A., 1968, Geology and petrography of the volcanic rocks south of Hawkins Basin, S.E. Idaho: Idaho State University M.S. thesis, 66 p.

Christiansen, R.L., 1984, Yellowstone magmatic evolution: Its bearing on understanding large volume explosive volcanism, *in* Explosive Volcanism: Inception, Evolution, Hazards: National Academy Press, Washington, D.C., p. 84-95.

Christiansen, R.L., and E.H. McKee, 1978, Late Cenozoic volcanic and tectonic evolution of the Great Basin and Columbia intermountain regions, *in* R.B. Smith and G.P. Eaton, eds., Cenozoic Tectonics and Regional Geophysics of the Western Cordillera: Geological Society of America Memoir 152, p. 283-311.

Cluer, J.K., and B.L. Cluer, 1986, The late Cenozoic Camas Prairie rift, south-central Idaho: Contributions to Geology, University of Wyoming, v. 24, no. 1, p. 91-101.

Compton, R.R., 1983, Displaced Miocene rocks on the west flank of the Raft River-Grouse Creek core complex, Utah, *in* D.M. Miller, V.R. Todd, and K.A. Howard, eds., Tectonic and Stratigraphic Sudies in the Eastern Great Basin: Geological Society of America Memoir 157, p. 271-280.

Corbett, M.K., 1978, Geologic map of the northern Portneuf Range: U.S. Geological Survey Open-File Report 78-1018, scale 1:48,000.

Covington, H.R., 1983, Structural evolution of the Raft River basin, Idaho, *in* D.M. Miller, V.R. Todd, and K.A. Howard, eds., Tectonic and Stratigraphic Sudies in the Eastern Great Basin: Geological Society of America Memoir 157, p. 229-238.

Cress, L.D., 1981, Stratigraphy and structure of the south half of the Deep Creek Mountains, Oneida and Power counties, Idaho: Colorado School of Mines Ph.D. dissertation, 251 p.

Dixon, J.S., 1980, Regional structural synthesis, Wyoming salient of western Overthrust Belt: American Association of Petroleum Geologists Bulletin, v. 66, p. 1560-1580.

Doherty, D.J., L.A. McBroome, and M.A. Kuntz, 1979, Preliminary geologic interpretation and lithological log of the exploratory test well (INEL-1), Idaho National Engineering Laboratory, eastern Snake River Plain, Idaho: U.S. Geological Survey Open-File Report 79-1248, 10 p.

Eaton, G.P., R.R. Wahl, H.L. Prostka, D.R. Mabey, and M.D. Kleinkopf, 1978, Regional gravity and tectonic patterns: Their relation to late Cenozoic epeirogeny and lateral spreading in the western Cordillera, *in* R.B. Smith and G.P. Eaton, eds., Cenozoic Tectonics and Regional Geophysics of the Western Cordillera: Geological Society of America Memoir 152, p. 51-92.

Ekren, E.B., D.H. McIntyre, and E.H. Bennett, 1984, High-temperature, large volume, lavalike ash-flow tuffs without calderas in southwestern Idaho: U.S. Geological Survey Professional Paper 1272, 73 p.

Ekren, E.B., D.H. McIntyre, E.H. Bennett, and R.F. Marvin, 1982, Cenozoic stratigraphy of western Owyhee countty, Idaho, *in* Bill Bonnichsen and R.M. Breckenridge, eds., Cenozoic Geology of

Idaho: Idaho Bureau of Mines and Geology Bulletin 26, p. 215-236.

Embree, G.F., L.A. McBroome, and D.J. Doherty, 1982, Preliminary stratigraphic framework of the Pliocene and Miocene rhyolites, eastern Snake River Plain, Idaho, *in* Bill Bonnichsen and R.M. Breckenridge, eds., Cenozoic Geology of Idaho: Idaho Bureau of Mines and Geology Bulletin 26, p. 333-334.

England, P., and P. Molnar, 1990, Surface uplift, uplift of rocks, and exhumation of rocks: Geology, v. 18, p. 1173-1177.

Fritz, W.J., and J.W. Sears, 1993, Tectonics of the Yellowstone hotspot wake in southwestern Montana: Geology, v. 21, p. 427-430.

Garmezy, Larry, 1981, Geology and tectonic evolution of the southern Beaverhead Range, east-central Idaho: Pennsylvania State University M.S. thesis, 155 p.

Geslin, J.K., P.K. Link, J.W. Riesterer, M.A. Kuntz, and C.M. Fanning, 2002, Pliocene and Quaternary stratigraphic architecture and drainage systems of the Big Lost trough, northeastern Snake River Plain, Idaho, *in* P.K. Link and L.L. Mink, eds., Geology, Hydrogeology, and Environmental Remediation: Idaho National Engineering and Environmental Laboratory, Eastern Snake River Plain, Idaho: Geological Society of America Special Paper 353, p. 11-26.

Greensfelder, R.W., 1981, Lithospheric structure of the eastern Snake River Plain, Idaho: Stanford University Ph.D. dissertation, 188 p.

Gripp, A.E., and R.G. Gordan, 1990, Current plate velocities relative to hot-spots incorporating the NUVEL-1 global plate motion model: Geophysical Research Letters, v. 17, p. 1109-1112.

Hackett, W.R., M.H. Anders, and R.C. Walter, 1994, Preliminary stratigraphic framework of rhyolites from corehole WO-2, Idaho National Engineering Laboratory: Caldera-related, late-Tertiary silicic volcanism of the eastern Snake River Plain (abs.): Proceedings of the VII International Symposium on the observation of the continental crust through drilling: International Continental Drilling Program, Santa Fe, New Mexico, unpaginated.

Hackett, W.R., S.M. Jackson, and R.P. Smith, 1996, Paleoseismology of volcanic environments, *in* J.P. McCalpin, ed., Paleoseismology: Academic Press, New York, p. 147-182.

Hamilton, Warren, 1989, Crustal geologic processes of the United States, *in* L.C. Pakiser and W.D. Mooney, eds., Geophysical Framework of the Continental United States: Geological Society of America Memoir 172, p. 743-781.

———, 1987, Plate-tectonic evolution of the western U.S.A.: Episodes, v. 10, p. 271-276.

Henderson, E.P., 1991, Neogene basin filling of Goose Creek basin, south-central Idaho, northwestern Utah, and northeastern Nevada: Geological Society of America Abstracts with Programs, v. 23, no.4, p. 32.

Hildebrand, R.T., and K.R. Newman, 1985, Miocene sedimentation in the Goose Creek basin, south-central Idaho, northeastern Nevada, and northwestern Utah, *in* R.M. Flores and S.S. Kaplan, eds., Cenozoic Paleogeography of West-Central United States: Society of Economic Paleontologists and Mineralogists, Rocky Mountain Section, Symposium 3, p. 55-70.

Hladky, F.R., 1986, Geology of an area north of the narrows of Ross Fork Canyon, northernmost Portneuf Range, Fort Hall Indian Reservation, Bannock and Bingham counties, Idaho: Idaho State University M.S. thesis, 110 p.

Hladky, F.R., and K.S. Kellogg, 1987, Geologic map of the western part of the Fort Hall Indian Reservation, Idaho: U.S. Geological Survey, Branch of Central Mineral Resources, 38 p.

Hodges, M.K.V., and D.W. Rodgers, 1999, Middle Miocene initiation of Basin-Range faulting and eastern Snake River Plain subsidence—evidence from east-central Idaho: Geological Society of America Abstracts with Programs, v. 31, no. 4, p. A-17.

Hough, B.G., 2001, Temporal constraints on crustal flexure adjacent to the eastern Snake River Plain, Idaho: Idaho State University M.S. thesis, 82 p.

Houser, B.B., 1992, Quaternary stratigraphy of an area northeast of American Falls Reservoir, eastern Snake River Plain, Idaho, *in* P.K. Link, M.A. Kuntz, and L.B. Platt, eds., Regional Geology of Eastern Idaho and Western Wyoming: Geological Society of America Memoir 179, p. 269-288.

Humphreys, E.D., K.G. Duecker, D.L. Schutt, and R.B. Smith, 1990, Beneath Yellowstone: Evaluating plume and nonplume models using teleseismic images of the upper mantle: GSA Today, v. 10, no. 12, p. 1-7.

Janecke, S.U., 1993, Estimates of late Cenozoic extension, east-central Idaho: Geological Society of America Abstracts with Programs, v. 25, no. 5, p. 56.

Janecke, S.U., M.E. Perkins, and R.B. Smith, 2000, Normal fault patterns around the Yellowstone hot spot: A new model: Geological Society of America Abstracts with Programs, v. 32, no. 7, p. A-45.

Kellogg, K.S., 1990, Geologic map of the south Putnam Mountain quadrangle, Bannock and Caribou counties, Idaho: U.S. Geological Survey Geologic Quadrangle Map GQ-1665, scale 1:24,000.

———, 1992, Cretaceous thrusting and neogene block rotation in the northern Portneuf Range region, southeastern Idaho, *in* P.K. Link, M.A. Kuntz, and L.B. Platt, eds., Regional Geology of Eastern Idaho and Western Wyoming: Geological Society of America Memoir 179, p. 95-113.

Kellogg, K.S., S.S. Harlan, H.H. Mehnert, L.W. Snee, K.L. Pierce, W.R. Hackett, and D.W. Rodgers, 1994, Major 10.2-Ma rhyolitic volcanism in the eastern Snake River Plain, Idaho—Isotopic age and stratigraphic setting of the Arbon Valley Tuff Member of the Starlight Formation: U.S. Geological Survey Bulletin 2091, 18 p.

Kellogg, K.S., and R.F. Marvin, 1988, New potassium-argon ages, geochemistry, and tectonic setting of upper Cenozoic volcanic rocks near Blackfoot, Idaho: U.S. Geological Survey Bulletin 1806, 19 p.

Kellogg, K.S., S.S. Oriel, R.E. Amerman, P.K. Link, and F.R. Hladky, 1989, Geologic map of the Jeff Cabin Creek quadrangle, Bannock and Caribou counties, Idaho: U.S. Geological Survey Geologic Quadrangle Map GQ-1669, scale 1:24,000.

King, Clarence, 1878, U.S. Geologic Exploration, Fortieth Parallel Report, v. 1, p. 412-440.

Kirkham, V.R.D., 1927, A geologic reconnaissance of Clark and Jefferson and parts of Butte, Custer, Fremont, Lemhi, and Madison counties, Idaho: Idaho Bureau of Mines and Geology Pamphlet 19, 47 p.

———, 1931, Snake River downwarp: Journal of Geology, v. 39, p. 456-487.

Kuntz, M.A., 1992, A model based perspective of basaltic volcanism, eastern Snake River Plain, Idaho, *in* P.K. Link, M.A. Kuntz, and L.B. Platt, eds., Regional Geology of Eastern Idaho and Western Wyoming: Geological Society of America Memoir 179, p. 289-304.

Kuntz, M.A., S.R. Anderson, D.E. Champion, M.A. Lanphere, and D.J. Grunwald, 2002, Tension cracks, eruptive fissures, dikes, and faults related to late Pliocene-Holocene basaltic volcanism and implication for the distribution of hydraulic conductivity in the eastern Snake River Plain, Idaho, *in* P.K. Link and L.L. Mink, eds., Geology, Hydrogeology, and Environmental Remediation: Idaho National Engineering and Environmental Laboratory, Eastern Snake River Plain, Idaho: Geological Society of America Special Paper 353, p. 111-134.

Kuntz, M.A., D.E. Champion, E.C. Spiker, R.H. Lefebvre, and L.A. McBroome, 1982, The Great Rift and evolution of the Craters of the Moon lava field, Idaho, *in* Bill Bonnichsen and R.M. Breckenridge, eds., Cenozoic Geology of Idaho: Idaho Bureau of Mines and Geology Bulletin 26, p. 423-437.

Kuntz, M.A., H.R. Covington, and L.J. Schoor, 1992, An overview of basaltic volcanism of the Eastern Snake River Plain, Idaho, *in* P.K. Link, M.A. Kuntz, and L.B. Platt, eds., Regional Geology of Eastern Idaho and Western Wyoming: Geological Society of America Memoir 179, p. 227-269.

Kuntz, M.A., Betty Skipp, M.A. Lanphere, W.E. Scott, K.L. Pierce, G.B. Dalrymple, D.E. Champion, G.F. Embree, W.R. Page, L.A. Morgan, R.P. Smith, W.R. Hackett, and D.W. Rodgers, 1994a, Geologic map of the Idaho National Engineering Laboratory and adjoining areas, eastern Idaho: U.S. Geological Survey Miscellaneous Investigations Map I-2330, scale 1:100,000.

Kuntz, M.A., Betty Skipp, W.E. Scott, and W.R. Page, 1984, Preliminary geologic map of the Idaho National Engineering Laboratory and adjoining areas: U.S. Geological Survey Open-File Report 84-281, 25 p.

Lageson, D.R., 1992, Possible Laramide influences on the Teton normal fault, western Wyoming, *in* P.K. Link, M.A. Kuntz, and L.B. Platt, eds., Regional Geology of Eastern Idaho and Western Wyoming: Geological Society of America Memoir 179, p. 183-196.

Leeman, W.P., 1982, Development of the Snake River Plain-Yellowstone Plateau province, Idaho and Wyoming: An overview and petrographic model, *in* Bill Bonnichsen and R.M. Breckenridge, eds., Cenozoic Geology of Idaho: Idaho Bureau of Mines and Geology Bulletin 26, p. 155-177.

LeFebre, G.B., 1984, Geology of the Chinks Peak area, Pocatello Range, Bannock County, Idaho: Idaho State University M.S. thesis, 61 p.

Love, J.D., 1977, Summary of Upper Cretaceous and Cenozoic stratigraphy and of tectonic and glacial events in Jackson Hole, northwestern Wyoming: Wyoming Geological Association 29th Annual Field Conference Guidebook, p. 585-594.

Love, J.D., J.C. Reed, and A.C. Christiansen, 1992, Geologic map of Grand Teton National Park, Teton County, Wyoming: U.S. Geological Survey Map I-2031, scale 1: 62,500.

Lowry, A.R., and R.B. Smith, 1995, Strength and rheology of the western U.S. Cordillera: Journal of Geophysical Research, v. 100, p. 17,947-17,963.

Mahoney, J.B., 1987, The geology of the northern Smoky Mountains and stratigraphy of a portion of the lower Permian Grand Prize Formation, Blaine and Camas counties, Idaho: Idaho State University M.S. thesis, 143 p.

Mansfield, G.R, 1927, Geography, geology and mineral resources of part of southeastern Idaho, with descriptions of Carboniferous and Triassic fossils by G.H. Girty: U.S. Geological Survey Professional Paper 152, 453 p.

McBroome, L.A., 1981, Stratigtraphy and origin of Neogene ash-flow tuffs on the northcentral margin of the eastern Snake River Plain, Idaho: University of Colorado M.S. thesis, 74 p.

McQuarrie, Nadine, 1997, Crustal flexure adjacent to the eastern Snake River Plain, Idaho: Idaho State University, M.S. thesis, 87 p.

McQuarrie, Nadine, and D.W. Rodgers, 1998, Subsidence of a volcanic basin by flexure and lower crustal flow: The eastern Snake River Plain, Idaho: Tectonics, v. 17, p. 203-220.

Miller, D.M., 1980, Structural geology of the northern Albion Mountains, south central Idaho, *in* M.D. Crittenden, P.J. Coney, and G.H. Davis, eds., Cordilleran Metamorphic Core Complexes: Geological Society of America Memoir 153, p. 399-423.

Morgan, L.A., D.J. Doherty, and W.P. Leeman, 1984, Ignimbrites of the eastern Snake River Plain: Evidence for major caldera-forming eruptions: Journal of Geophysical Research, v. 89, no. B10, p. 8665-8678.

Morgan, W.J., 1972, Plate motions and deep mantle convection: Geological Society of America Memoir 132, p. 7-22.

Mueller, K.J., and A.W. Snoke, 1993, Cenozoic basin development and normal fault systems associated with the exhumation of metamorphic complexes in northeastern Nevada, *in* M.M. Lahren, J.H. Trexler, Jr., and Claude Spinosa, eds., Crustal Evolution of the Great Basin and the Sierra Nevada: Cordilleran/Rocky Mountains Section, Geological Society of America Guidebook, Department of Geological Sciences, University of Nevada, Reno, p. 1-34.

Myers, W.B., and Warren Hamilton, 1964, Deformation accompanying the Hebgen Lake earthquake of August 17, 1959: U.S. Geological Survey Professional Paper 435, p. 55-98.

Mytton, J.W., P.L. Williams, and W.A. Morgan, 1990, Geologic map of the Stricker 4 quadrangle, Cassia, Twin Falls, and Jerome counties, Idaho: U.S. Geological Survey Miscellaneous Investigations Series Map I-2052, scale 1:48,000.

Nunn, J.A., and J.R. Aires, 1988, Gravity anomalies and flexure of the lithosphere at the Middle Amazon Basin, Brazil: Journal of Geophysical Research, v. 93, p. 415-428.

Oriel, S.S., and D.W. Moore, 1985, Geologic map of the west and east Palisades Roadless areas, Idaho and Wyoming: U.S. Geological Survey Miscellaneous Field Studies Map MF-1619-B, scale 1:50,000.

Oriel, S.S., and L.B. Platt, 1980, Geologic map of the Preston 1º x 2º quadrangle, southeastern Idaho and western Wyoming: U.S. Geological Survey Miscellaneous Investigation Series Map I-1127, scale 1:250,000.

Pankratz, L.W., and H.D. Ackermann, 1982, Structure along the northwest edge of the Snake River Plain interpreted from seismic refraction: Journal of Geophysical Research, v. 87, no. B4, p. 2676-2682.

Parsons, Tom, and G.A. Thompson, 1991, The role of magma overpressuring in suppressing earthquakes and topography: Worldwide examples: Science, v. 253, p. 1399-1402.

Parsons, Tom, G.A. Thompson, and R.P. Smith, 1998, More than one way to stretch: A tectonic model for extension along the plume track of the Yellowstone hot spot and adjacent Basin and Range Province: Tectonics, v. 17, p. 221-234.

Peng, Xiaohua, and E.D. Humphreys, 1998, Crustal velocity structure across the eastern Snake River Plain and the Yellowstone swell: Journal of Geophysical Research, v. 103, p. 7171-7186.

Perkins, M.E., and W.P. Nash, 1994, Tephrochronology of the Teewinot Formation, Jackson Hole, Wyoming: Geological Society of America Abstracts with Programs, v. 26, no. 6, p. 58-59.

Perkins, M.E., W.P. Nash, F.H. Brown, and R.J. Fleck, 1995, Fallout tuffs of Trapper Creek, Idaho—A record of Miocene explosive volcanism in the Snake River Plain volcanic province: U.S. Geological Survey Bulletin, v. 107, p. 1484-1506.

Pierce, K.L., H.R. Covington, P.L. Williams, and D.H. McIntyre, 1983, Geologic map of the Cotterel Mountains and the northern Raft River Valley, Cassia County, Idaho: U.S. Geological Survey Miscellaneous Investigation Series Map I-1450, scale 1:48,000.

Pierce, K.L., and L.A. Morgan, 1992, The track of the Yellowstone hotspot; volcanism, faulting and uplift, *in* P.K. Link, M.A. Kuntz, and L.B. Platt, eds., Regional Geology of Eastern Idaho and Western Wyoming: Geological Society of America Memoir 179, p. 1-53.

Pierce, K.L., and W.E. Scott, 1982, Pleistocene episodes of alluvial-gravel deposition, southeastern Idaho, *in* Bill Bonnichsen and R.M. Breckenridge, eds., Cenozoic Geology of Idaho: Idaho Bureau of Mines and Geology Bulletin 26, p. 685-702.

Pogue, K.R., 1984, Geology of the Mt. Putnam area, northern Portneuf Range, Bannock and Caribou counties, Idaho: Idaho State University M.S. thesis, 106 p.

Pratt, R.M., 1982, The case for lateral offset of the overthrust belt along the Snake River Plain, *in* R.B. Powers, ed., Geologic Studies of the Cordilleran Thrust Belt: Rocky Mountain Association of Geologists, v. 1, p. 235-246.

Reilinger, R.E., G.P. Citron, and L.D. Brown, 1977, Recent vertical crustal movements from precise leveling data in southwestern Montana, western Yellowstone National Park and the Snake River Plain: Journal of Geophysical Research, v. 82, p. 5349-5359.

Richins, R.D., J.C. Pechmann, R.B. Smith, C.J. Langer, S.K. Goter, J.E. Zwollweg, and J.J. King, 1987, The 1983 Borah Peak, Idaho, earthquake and its aftershocks: Bulletin of the Seismological Society of America, v. 77, no. 3, p. 694-723.

Rodgers, D.W., and M.H. Anders, 1990, Neogene evolution of Birch Creek Valley near Lone Pine, Idaho *in* Sheila Roberts, ed., Geologic Field Tours of Western Wyoming and Parts of Adjacent Idaho, Montana, and Utah: Geological Survey of Wyoming Public Information Circular 29, p. 27-40.

Rodgers, D.W., Mason Estes, Chris Meehan, Terrence Osier, John Preacher, and Ian Warren, 1994, Style, kinematics, and timing of Neogene-Quaternary extension in the northeastern Basin and Range: Geological Society of America Abstracts with Programs, v. 75, p. 61.

Rodgers, D.W., W.R. Hackett, and H.T. Ore, 1990, Extension of the Yellowstone Plateau, eastern Snake River Plain, and Owyhee Plateau: Geology, v. 18, p. 1138-1141.

Rodgers, D.W., and S.U. Janecke, 1992, Tertiary paleogeographic maps of the western Idaho-Wyoming-Montana thrust belt, *in* P.K. Link, M.A. Kuntz, and L.B. Platt, eds., Regional Geology of Eastern Idaho and Western Wyoming: Geological Society of America Memoir 179, p. 83-94.

Rodgers, D.W., P.K. Link, and A.D. Huerta, 1995, Structural framework of mineral deposits hosted by Paleozoic rocks in the northeastern part of the Hailey 1º x 2º quadrangle, south-central Idaho: U.S. Geological Survey Bulletin 2064-B, 18 p.

Rodgers, D.W., and K.L. Othberg, 1999, Geologic map of the Pocatello South quadrangle, Idaho: Idaho Geological Survey Geologic Map 26, scale 1:24,000.

Rodgers, D.W., and N.C. Zentner, 1988, Fault geometries along the northern margin of the eastern Snake River Plain, Idaho: Geological Society of America Abstracts with Programs, v. 20, p. 465.

Royse, Frank, Jr., M.A. Warner, and D.L. Reese, 1975, Thrust belt structural geometry and related stratigraphic problems, Wyoming-Idaho-northern Utah, *in* D.W. Bolyard, ed., Deep Drilling Frontiers of the Central Rocky Mountains: Rocky Mountains Association of Geologists Symposium, Denver, Colorado, p. 41-54.

Ruppel, E.T., 1967, Late Cenozoic drainage reversal, east-central Idaho, and its relation to possible undiscovered placer deposits: Economic Geology, v. 61, p. 648-663.

Rytuba, J.J., and E.H. McKee, 1984, Peralkaline ash flow tuffs and calderas of the McDermitt volcanic field, southeast Oregon and northcentral Nevada: Journal of Geophysical Research, v. 89, p. 8616-8628.

Saltzer, S.D., and K.V. Hodges, 1988, The Middle Mountain shear zone, southern Idaho—Kinematic analysis of an early Tertiary high-temperature detachment: Geological Society of America Bulletin, v. 100, p. 96-103.

Saltzer, R.L., and E.D. Humphreys, 1997, Upper mantle P-wave velocity structure of the eastern Snake River Plain and its relationship to geodynamic models of the region: Journal of Geophysical Research, v. 102, p. 11,829-11,841.

Schmidt, D.L., 1962, Quaternary geology of the Bellevue area in Blaine and Camas counties, Idaho: U.S. Geological Survey Open-File Report 625, 133 p.

Scott, W.E., 1982, Surficial geologic map of the eastern Snake River Plain and adjacent area, 111º to 115ºW, Idaho and Wyoming: U.S. Geological Survey Miscellaneous Investigations Map I-1372, scale 1:125,000.

Scott, W.E., K.L. Pierce, and M.H. Hait, Jr., 1985, Quaternary tectonic setting of the 1983 Borah Peak earthquake, central Idaho, *in* R.S. Stein and R.C. Bucknam, eds., Proceedings, Workshop XXVIII on the Borah Peak, Idaho, Earthquake: U.S. Geological Survey Open-File Report 85-290, p. 1-16.

Sengor, A.M.C., 1995, Sedimentation and tectonics of fossil rifts, *in* C.J. Busby and R.V. Ingersoll, eds., Tectonics of Sedimentary Basins: Blackwell Science, Cambridge, Massachusettes, p. 53-118.

Skipp, Betty, 1988, Geologic map of Mackay 4 (Grouse) NE quadrangle, Butte and Custer counties, Idaho: U.S. Geological Survey Open-File report 88-423, scale 1:24,000.

Skipp, Betty, and D.D. Bollmann, 1992, Geologic map of Blizzard Mountain North quadrangle, Butte and Custer counties, Idaho: U.S. Geological Survey Open-File Report 92-280, scale 1:24,000.

Skipp, Betty, M.A. Kuntz, and L.A. Morgan, 1990, Geologic map of Mackay 4 (Grouse) SE quadrangle, Butte and Custer counties, Idaho: U.S. Geological Survey Open-File Report 89-431, scale 1:24,000.

Skipp, Betty, H.J. Prostka, and D.L. Schleicher, 1979, Preliminary geologic map of the Edie Ranch quadrangle, Clark County, Idaho, and Beaverhead County, Montana: U.S. Geological Survey Open-File Report 79-845, scale 1:62,500.

Smith, C.L., 1966, Geology of the eastern Mount Bennett Hills, Camas, Gooding, and Lincoln counties, Idaho: University of Idaho Ph.D. dissertation, 129 p.

Smith, R.B., W.D. Richins, and D.I. Doser, 1985, The 1983 Borah Peak, Idaho, earthquake: Regional seismicity, kinematics of faulting and tectonic mechanism, *in* R.S. Stein and R.C. Bucknam, eds., Proceedings, Workshop XXVIII on the Borah Peak, Idaho, Earthquake: U.S. Geological Survey Open-File Report 85-290, p. 236-263.

Smith, R.B., and N.L. Sbar, 1974, Contemporary tectonics and seismicity of the western United States with emphasis on the Intermountain Seismic Belt: Geological Society of America Bulletin, v. 85, p. 1205-1218.

Smith, R.B., M.M. Schilly, L.W. Braile, J. Ansorge, J.L. Lehman, M.R. Baker, C. Prodehl, J.H. Healy, S. Mueller, and R.W. Greensfelder, 1982, The 1978 Yellowstone-eastern Snake River Plain seismic profiling experiment: Crustal structure of the Yellowstone region and experiment design: Journal of Geophysical Research, v. 87, no. B4, p. 2583-2596.

Sparlin, M.A., L.W. Braile, and R.B. Smith, 1982, Crustal structure of the eastern Snake River Plain determined from ray trace modeling of seismic refraction data: Journal of Geophysical Research, v. 87, no. B4, p. 2619-2633.

Suppe, John, Christine Powell, and Robert Berry, 1975, Regional topography, seismicity, Quaternary volcanism, and the present-day tectonics of the western United States: American Journal of Science, v. 275A, p. 397-436.

Trimble, D.E., 1980, Geology of the Michaud and Pocatello quadrangles, Bannock and Power counties, Idaho: U.S. Geological Survey Bulletin 1400, 88 p.

Trimble, D.E., and W.J. Carr, 1976, Geology of the Rockland and Arbon quadrangles, Power County, Idaho: U.S. Geological Survey Bulletin 1399, 115 p.

Turcotte, D.L., and Gerald Schubert, 1982, Geodynamics: Applications of Continuum Physics to Geological Problems: John Wiley and Sons, New York, 450 p.

Turko, J.M., and P.L.K. Knuepfer, 1991, Late Quaternary fault segmentation from analysis of scarp morphology: Geology, v. 19, p. 718-721.

Waldrop, H.A., 1975, Surficial geologic map of the Henry's Lake quadrangle, Idaho and Montana: U.S. Geological Survey Miscellaneous Investigations Map I-684.

Williams, P.L., H.R. Covington, and K.L. Pierce, 1982, Cenozoic stratigraphy and tectonic evolution of the Raft River Basin, Idaho, *in* Bill

Bonnichsen and R.M. Breckenridge, eds., Cenozoic Geology of Idaho: Idaho Bureau of Mines and Geology Bulletin 26, p. 491-504.

Williams, P.L., J.W. Mytton, and H.R. Covington, 1990, Geologic map of the Stricker 1 quadrangle, Cassia, Twin Falls, and Jerome counties, Idaho: U.S. Geological Survey Miscellaneous Investigations Map I-2078, scale 1:48,000.

Witkind, I.J., 1972, Geologic map of the Henry's Lake quadrangle, Idaho and Montana: U.S. Geological Survey Map I-781-A, scale 1:48,000.

———, 1976, Geologic map of the southern part of the Upper Red Rock Lake quadrangle, southwest Montana and adjacent Idaho: U.S. Geological Survey Miscellaneous Investigations Map I-943, scale 1:48,000.

Woodward, N.B., 1986, Thrust fault geometry of the Snake River Range, Idaho and Wyoming: Geological Society of America Bulletin, v. 97, p. 178-193.

Zentner, N.C., 1989, Neogene normal faults related to the structural origin of the eastern Snake River Plain, Idaho: Idaho State University M.S. thesis, 47 p.

Zoback, M.L., and G.A. Thompson, 1978, Basin and Range rifting in northern Nevada: Clues from a mid-Miocene rift and its subsequent offsets: Geology, v. 6, p. 111-116.

Zoback, M.L., and Mark Zoback, 1980, State of stress in the conterminous United States: Journal of Geophysical Research, v. 85, no. B11, p. 6113-6156.